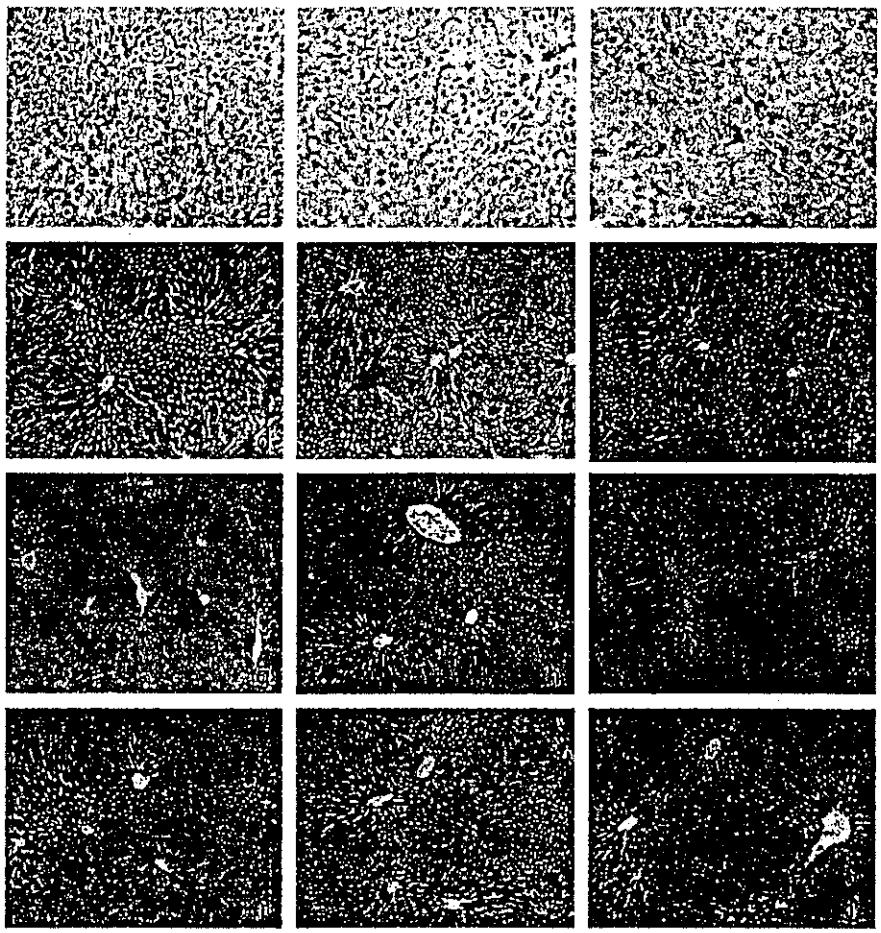

Fig. 3. Immunohistochemical distribution of CY1A1 (a–c), CYP2C6 (d–f), CYP2E1 (g–i), and CYP3A1 (j–l) proteins in the liver of nonpregnant rats (a, d, g, and j), midpregnant rats (b, e, h, and k), and late pregnant rats (c, f, i, and l). Immunostaining, magnification ×100.

CYP2E1 in rat liver peroxisomes by a mechanism of ischemia/reperfusion-induced oxidative stress. Decreases in CYP 1A1 and CYP2E1 protein levels in rat late pregnancy were also observed in the present study. Reduction of hepatic CYPs mRNAs expression during oxidative stress may be part of and adaptive response by the liver to minimize cell damage (Barke et al., 1994). To our knowledge, the relationship between CYPs expression and oxidative stress during pregnancy has not been investigated. It remains to be determined what extent changes in hepatic CYPs expression are regulated by increased oxidative stress during pregnancy.

Endogenous nitric oxide (NO), a potent vasodilator and a platelet antiaggregating factor, might also be involved in down-regulation of hepatic CYPs expression during rat pregnancy. Evidences provided by Conrad et al. (1993), McLaughlin and Conrad (1995), and Xu et al. (1996) show that the biosynthesis of NO increases during rat gestation as determined with plasma level and urinary excretion. Increased NO production has been suggested to play a role in the hemodynamic alterations of pregnancy (Xu et al., 1996). As one of the oxidative stresses, an increase in NO could also be thought to be an adaptive response during pregnancy by inhibiting CYP450 expression. Using human hepatocytes as an experimental model, Gonzalez (1990) demonstrated that exogenously added NO inhibited the CYP1A2 activity. In liver extracts, NO decreased the mRNA and protein expression of the phenobarbital-inducible CYP2B1 and CYP2B2 (Khatsenko et al., 1997), and it also decreased the constitutive expression of CYP3A2 (Minamiyama et al., 1997). In rat hepatocytes, high concentrations of bacterial lipopolysaccharide (LPS) evoked

Table 2
Distribution and degree of immunostainability for CYPs in the liver

CYPs	Cell type	
	Hepatocytes	Endothelial cells of sinusoids and veins
CYP1A1	–	++
CYP2B1/2	+	–
CYP2C6	++	–
CYP2C12	+++	–
CYP2D1	+++	–
CYP2D4	–	–
CYP2E1	++	–
CYP3A1	+++	–
CYP4A1	±	±

Note: –, negative; ±, very slight; +, slight; ++, moderate; +++, marked.

a rapid down-regulation of phenobarbital-induced CYP2B1 protein that was NO-dependent (Ferrari et al., 2001). Moreover, in a very recent study (Wang et al., 2003), it was demonstrated that a decrease in renal microsomal CYP4A1/CYP4A3 expression is dependent on NO in rat late pregnancy. These results, down-regulations of CYP2B1, CYP2B2, and CYP4A1 induced by NO, are partially consistent with our data. Therefore, these observations raise the possibility that NO may participate in down-regulation of hepatic CYPs during rat pregnancy. To date, it remains to be assessed that NO is involved in regulation of hepatic CYPs during rat pregnancy.

Pregnancy is a dynamic condition with major endocrine and physiological changes. At the present time, it is not clear how pregnancy regulates CYP450 expression. The abovementioned and other unknown mechanisms may be operating together to some extent, resulting in the decreased CYP450 expression. However, it should be pointed out that some CYPs were not affected during rat pregnancy, at least in the present study.

The localization and distribution of the CYP1A1, CYP2B1/2B2, CYP2C6, CYP2C12, CYP2D1, CYP2D4, CYP2E1, CYP3A1, and CYP4A1 proteins in the rat liver were also investigated by using immunohistochemistry with anti-CYPs antibodies. We observed that CYP1A1 is expressed in endothelial cells of both sinusoids and veins in the liver. The localization of CYP1A1 observed here confirms the findings of Annas and Brittebo (1998) who reported a colocalization of CYP1A1 immunoreactivity and covalent binding of 3H-Trp-P-1 in endothelial linings of capillaries and veins of heart, skeletal, muscle, and uterus in β-naphthoflavone (BNF)-treated rodents. Thus, endothelial cells appear to be the main cell type that expresses CYP1A1 in the rat liver. It has been suggested that CYP1A1 may be a factor in the regulation of vascular tone at these sites (Annas and Brittebo, 1998). CYP2B1/2B2, CYP2C6, CYP2C12, CYP2D1, CYP2E1, CYP3A1, and CYP4A1 were mainly expressed in centrilobular hepatocytes of hepatic acinus. This supports the general knowledge that most CYPs are expressed mainly in this region and some of them throughout the acinus in the rat liver. CYP4A1 was also detected in endothelial cells of both sinusoids and veins. We failed to show the CYP2D4 proteins in either pregnant or nonpregnant rat liver by using immunohistochemical staining.

In conclusion, the present study showed that pregnancy was associated with down-regulation of protein levels of CYP1A1, CYP2B1/2B2, CYP2C6, CYP2E1, and CYP4A1 in the rat liver but did not affect those of CYP2C12, CYP2D1, and CYP3A1. CYP1A1 and CYP4A1, especially the former, were expressed in endothelial cells of both sinusoids and veins. We are now conducting the study on the potential effects of oxidative stress and nitric oxide on the regulation of CYPs during pregnancy.

References

Annas, A., Brittebo, E.B., 1998. Localization of cytochrome P4501A1 and covalent binding of a mutagenic heterocyclic amine in blood vessel endothelia of rodents. Toxicology 129, 145–156.

Barker, C.W., Fagan, J.B., Pasco, D.S., 1994. Down-regulation of P4501A1 and P4501A2 mRNA expression in isolated hepatocytes by oxidative stress. J. Biol. Chem. 269, 3985–3990.

Borlakoglu, J.T., Scott, A., Henderson, C.J., Wolf, C.R., 1993. Alterations in rat hepatic drug metabolism during pregnancy and lactation. Biochem. Pharmacol. 46, 29–36.

Casazza, J.P., Sohn, D.H., Park, K.S., Song, B.J., 1994. Serum acetone and liver acetone monooxygenase activity in pregnant rats, fetuses, and neonates: reversible pretranslational reduction of cytochrome P450IIE1 (P450IIE1) during pregnancy. Arch. Biochem. Biophys. 309, 111–116.

Conrad, K.P., Joffe, G.M., Kruszyna, H., Kruszyna, R., Rochelle, L.G., Smith, R.P., Chavez, J.E., Mosher, M.D., 1993. Identification of increased nitric oxide biosynthesis during pregnancy in rats. FASEB J. 7, 566–571.

Czekaj, P., Wiaderkiewicz, A., Florek, E., Wiaderkiewicz, R., 2000. Expression of cytochrome CYP2B1/2 in nonpregnant, pregnant and fetal rats exposed to tobacco smoke. Acta Biochim. Pol. 47, 1115–1127.

Dean, M.E., Stock, B.H., 1975. Hepatic microsomal metabolism of drugs during pregnancy in the rat. Drug Metab. Dispos. 3, 325–331.

Dean, M.E., Stock, B.H., 1989. The influence of phenobarbital administration on hepatic monooxygenase activity at various stages of gestation in the rat. Drug Metab. Dispos. 17, 579–581.

Ejiri, N., Katayama, K.I., Nakayama, H., Doi, K., 2001. Expression of cytochrome P450 (CYP) isozymes in rat placenta through pregnancy. Exp. Toxicol. Pathol. 53, 387–391.

Ejiri, N., Katayama, K., Doi, K., 2003. Induction of CYP3A1 by dexamethasone and pregnenolone-16 alpha-carbonitrile in pregnant rat and fetal livers and placenta. Exp. Toxicol. Pathol. 54, 273–279.

Ferrari, L., Peng, N., Halpert, J.R., Morgan, E.T., 2001. Role of nitric oxide in down-regulation of CYP2B1 protein, but not RNA, in primary cultures of rat hepatocytes. Mol. Pharmacol. 60, 209–216.

Feuer, G., 1979. Action of pregnancy and various progesterones on hepatic microsomal activities. Drug Metab. Rev. 9, 147–169.

Feuer, G., Kardish, R., 1975. Hormonal regulation of drug metabolism during pregnancy. Int. J. Clin. Pharmacol. Biopharm. 11, 366–374.

Feuer, G., Liscio, A., 1969. Origin of delayed development of drug metabolism in the newborn rat. Nature 223, 68–70.

Gatti, S., Faggioni, R., Echtenacher, B., Ghezzi, P., 1993. Role of tumour necrosis factor and reactive oxygen intermediates in lipopolysaccharide-induced pulmonary oedema and lethality. Clin. Exp. Immunol. 91, 456–461.

Gonzalez, F.J., 1990. Molecular genetics of the P-450 super family. Pharmacol. Ther. 45, 1–38.

Guarino, A.M., Gram, T.E., Schroeder, D.H., Call, J.B., Gillette, J.R., 1969. Alterations in kinetic constants for hepatic microsomal aniline hydroxylase and ethylmorphine *N*-demethylase associated with pregnancy in rats. J. Pharmacol. Exp. Ther. 168, 224–228.

Khatsenko, O.G., Boobis, A.R., Gross, S.S., 1997. Evidence for nitric oxide participation in down-regulation of CYP2B1/2 gene expression at the pretranslational level. Toxicol. Lett. 90, 207–216.

Liu, P.T., Kentish, P.A., Symons, A.M., Parke, D.V., 1993. The effects of ether anaesthesia on oxidative stress in rats—dose response. Toxicology 80, 37–49.

Mannering, G.J., Deloria, L.B., 1986. The pharmacology and toxicology of the interferons: an overview. Ann. Rev. Pharmacol. Toxicol. 26, 455–515.

McLaughlin, M.K., Conrad, K.P., 1995. Nitric oxide biosynthesis during pregnancy: implications for circulatory changes. Clin. Exp. Pharmacol. Physiol. 22, 164–171.

Miller, M.S., Warner, S.P., Jorquera, R., Castonguay, A., Schuller, H.M., 1992. Expression of the cytochrome P4502E and 2B gene families in the lungs and livers of nonpregnant, pregnant, and fetal hamsters. Biochem. Pharmacol. 44, 797–803.

Minamiyama, Y., Takemura, S., Imaoka, S., Funae, Y., Tanimoto, Y., Inoue, M., 1997. Irreversible inhibition of cytochrome P450 by nitric oxide. J. Pharmacol. Exp. Ther. 283, 1479–1485.

Mover-Lev, H., Ar, A., 1997. Changes in enzymatic antioxidant activity in pregnant rats exposed to hyperoxia or hypoxia. Comp. Biochem. Physiol. 118, 353–359.

Neale, M.G., Parke, D.V., 1973. Effects of pregnancy on the metabolism of drugs in the rat and rabbit. Biochem. Pharmacol. 22, 1451–1461.

Nelson, D.R., Koymans, L., Kamataki, T., Stegeman, J.J., Feyereisen, R., Waxman, D.J., Waterman, M.R., Gotoh, O., Coon, M.J., Estabrook, R.W., Gunsalus, I.C., Nebert, D.W., 1996. P450 superfamily: update on new sequences, gene mapping, accession numbers and nomenclature. Pharmacogenetics 6, 1–42.

Pahan, K., Smith, B.T., Singh, A.K., Singh, I., 1997. Cytochrome P-450 2E1 in rat liver peroxisomes: downregulation by ischemia/reperfusion-induced oxidative stress. Free Radical Biol. Med. 23, 963–971.

Peristeris, P., Clark, B.D., Gatti, S., Faggioni, R., Mantovani, A., Mengozzi, M., Orencole, S.F., Sironi, M., Ghezzi, P., 1992. *N*-acetylcysteine and glutathione as inhibitors of tumor necrosis factor production. Cell. Immunol. 140, 390–399.

Rogers, J.F., Nafziger, A.N., Bertino Jr., J.S., 2002. Pharmacogenetics affects dosing, efficacy, and toxicity of cytochrome P450-metabolized drugs. Am. J. Med. 113, 746–750.

Starkel, P., Laurent, S., Petit, M., Van Den Berge, V., Lambotte, L., Horsmans, Y., 2000. Early down-regulation of cytochrome P450 3A and 2E1 in the regenerating rat liver is not related to the loss of liver mass or the process of cellular proliferation. Liver 20, 405–410.

Sugino, N., Nakamura, Y., Takeda, O., Ishimatsu, M., Kato, H., 1993. Changes in activities of superoxide dismutase and lipid peroxide in corpus luteum during pregnancy in rats. J. Reprod. Fertil. 97, 347–351.

Symons, A.M., Turcan, R.G., Parke, D.V., 1982. Hepatic microsomal drug metabolism in the pregnant rat. Xenobiotica 12, 365–374.

Wadelius, M., Darj, E., Frenne, G., Rane, A., 1997. Induction of CYP2D6 in pregnancy. Clin. Pharmacol. Ther. 62, 400–407.

Wang, M.H., Wang, J., Chang, H.H., Zand, B.A., Jiang, M., Nasjletti, A., Laniado-Schwartzman, M., 2003. Regulation of renal CYP4A expression and 20-HETE synthesis by nitric oxide in pregnant rats. Am. J. Physiol.: Renal. Physiol. 285, F295–F302.

Xu, D.L., Martin, P.Y., St. John, J., Tsai, P., Summer, S.N., Ohara, M., Kim, J.K., Schrier, R.W., 1996. Upregulation of endothelial and neuronal constitutive nitric oxide synthase in pregnant rats. Am. J. Physiol. 271, R1739–R1745.

BIOLOGY OF REPRODUCTION 70, 1762–1767 (2004)
Published online before print 6 February 2004.
DOI 10.1095/biolreprod.103.026252

Involvement of p53 in 1-β-D-Arabinofuranosylcytosine-Induced Trophoblastic Cell Apoptosis and Impaired Proliferation in Rat Placenta

Hirofumi Yamauchi,[1] Kei-ichi Katayama, Masaki Ueno, Koji Uetsuka, Hiroyuki Nakayama, and Kunio Doi

Department of Veterinary Pathology, Graduate School of Agricultural and Life Sciences, The University of Tokyo, Tokyo 113-8657, Japan

ABSTRACT

1-β-D-Arabinofuranosylcytosine (Ara-C), a DNA-damaging agent, severely inhibits fetal growth and has teratogenicity. Recently, we reported that Ara-C also causes placental growth retardation and increases placental apoptosis. The aim of the present study is to elucidate the mechanisms of placental injury induced by genotoxic stress and involvement of p53, which mediates apoptosis and cell-cycle arrest after DNA damage. We injected Ara-C into pregnant rats on Day 13 of gestation and examined the placentas from 1 to 48 h after the administration. Terminal deoxynucleotidyltransferase-mediated dUTP end-labeling (TUNEL) revealed that the apoptosis of trophoblastic cells in the placental labyrinth zone increased from 3 h after the treatment and peaked at 6 h before returning to control levels at 48 h. An increase in cleaved caspase-3 immunoreactivity was also detected at 6 h. Proliferative activity as measured by immunohistochemistry for topoisomerase IIα and by mitotic index significantly decreased after the treatment in the labyrinth zone. Immunoreactivity for p53 protein in the placental labyrinth zone was remarkably enhanced and peaked at 3 h after treatment, although no increase in *p53* mRNA expression was detected with a reverse transcription-polymerase chain reaction. Regarding p53 target genes, *p21*, *cyclinG1*, and *fas* mRNA levels increased significantly and peaked at around 9 h after the treatment. These results indicate that Ara-C would induce apoptosis and impair cell proliferation in the placental labyrinth zone, and p53 and its transcriptional target genes may play an important role in the pathogenesis of the Ara-C-induced placental toxicity.

apoptosis, conceptus, placenta, toxicology, trophoblast

INTRODUCTION

Adequate placental growth and development are crucial to the development of the fetus, and dysfunctions of the placenta may be closely related to fetal developmental disabilities [1]. In the placenta during normal pregnancy in humans and experimental animals, apoptosis is observed in various kinds of component cells and is thought to play physiological roles in placental growth, turnover, and parturition [2–5]. In contrast, increased apoptosis is reported in human placenta complicated with intrauterine growth retardation or other abnormal pregnancies [6–10]. In experimental animals, placental apoptosis is induced concomitant with developmental disabilities such as fetal growth retardation, preterm delivery, and increased resorptions by the administration of N^G-nitro-L arginine methyl ester [11], lipopolysaccharides [12], and glucocorticoids [5] to dams. Thus, the placenta is thought to be susceptible to endocrinological abnormality, inflammatory cytokines, and oxidative stress, and increased placental apoptosis may cause placental dysfunction, resulting in abnormal fetal development.

Embryos and fetuses are vulnerable to genotoxic stress such as DNA damaging agents or radiation, and congenital anomalies are easily induced [13–16]. Genotoxic stress induces apoptosis and cell-cycle arrest in fetal tissues in a p53-dependent way, and this is recognized as a cause of congenital anomalies [15, 17–19]. The *p53*, a tumor suppressor gene, is involved in the regulation of apoptosis and cell-cycle arrest after DNA damage mainly through the transcriptional activation of its target genes, thereby preventing the propagation of damaged cells in a number of different paradigms [20].

However, little attention has been given to the effect of genotoxic stress on the placenta. Recently, ethylnitrosourea, a teratogenic DNA alkylating agent, was reported to induce apoptosis and growth arrest in trophoblastic cells in the placental labyrinth zone with the up-regulation of p53 protein in vivo [21]. 1-β-D-Arabinofuranosylcytosine (Ara-C), a cytidine analogue, is also known as a DNA-damaging agent. Ara-C is used in the clinical treatment for myelogenous leukemia and is associated with fetal growth restrictions and malformations such as microtis, auditory canal atresia, digit anomalies, and lower limb defects in humans [22–24]. It has a teratogenic effect and causes fetal growth retardation also in experimental animals [13, 25, 26]. Previously, we demonstrated that the administration of Ara-C to pregnant rats caused significant decreases of placental weight and thickness of the labyrinth zone with a marked increase in the number of apoptotic cells among trophoblastic cells of the placental labyrinth zone and confirmed that fetal weight was also restricted at 48 h after the administration [27].

The aim of the present study was to investigate the toxic effect of Ara-C in detail and to explore the mechanisms of increased apoptosis and growth inhibition in the placental labyrinth zone. For this purpose, we injected Ara-C into pregnant rats and investigated the sequential changes in the incidence of apoptotic cell death and kinetics of proliferative activity in the placental labyrinth zone histopathologically. In addition, to clarify the involvement of p53 in Ara-C-induced placental toxicity, we examined the sequential expression patterns of p53 protein and the mRNA of *p53* and its transcriptional target genes.

[1]Correspondence: Hirofumi Yamauchi, Department of Veterinary Pathology, Graduate School of Agricultural and Life Sciences, The University of Tokyo, 1-1-1 Yayoi, Bunkyo-ku, 113-8657 Tokyo, Japan.
FAX: 81 3 5841 8185; e-mail: yamauchi-h@umin.ac.jp

Received: 5 December 2003.
First decision: 29 December 2003.
Accepted: 3 February 2004.

ISSN: 0006-3363. http://www.biolreprod.org

TABLE 1. Primer sequences, cycle numbers, and accession numbers.

Gene	Sense primer	Antisense primer	Cycle number	Accession number
p53	ATATGAGCATCGAGCTCCCTCT	CACAACTGCACAGGGCATGT	29	X13058
p21	AAGTATGCCGTCGTCTGTTCG	GGCACTTCAGGGCTTTCTCTT	28	L41275
cyclinG1	GTGTCGGACTGAGCTGCTTTT	TTGGGAGGTGGGTTATCCTGT	25	X70871
fas	AAGAGGAGCGTTCGTGAAACC	GATCAGCAGCCAAAGGAGCTTA	31	D26112
GAPDH	GCTTCACCACCTTCTTGATGTC	GAGTATGTCGTGGAGTCTACTG	21	AF106860

MATERIALS AND METHODS

Animals and Chemicals

Pregnant Slc:Wistar rats (plug day: Day 0 of gestation) were obtained from Japan SLC Inc. (Shizuoka, Japan). They were kept under controlled conditions (temperature, 23 ± 2°C; relative humidity, 55% ± 5%) using an isolator caging system (Niki Shoji Co., Tokyo, Japan) and were fed commercial pellets (MF, Oriental Yeast Co., Tokyo, Japan) and water ad libitum. Ara-C (Sigma, St. Louis, MO) was dissolved in PBS and its concentration was adjusted to 50 mg/ml. The protocol of the present study was approved by the Animal Care and Use Committee of the Graduate School of Agricultural and Life Sciences, The University of Tokyo.

Treatments

Pregnant rats were injected intraperitoneally (i.p.) with 250 mg/kg of Ara-C on Day 13 of gestation (GD13). Under the conditions of this experiment, congenital anomalies and growth retardation were detected at a high rate in perinatal fetuses, although the incidence of fetal death was not markedly increased [25, 26]. At 1, 3, 6, 9, 12, 24, and 48 h after the treatment, six dams each were killed by heart puncture under ether anesthesia, and the placentas were collected. As controls, six pregnant rats were injected i.p. with an equivalent volume of PBS on GD13 and killed at the same time point as Ara-C-treated groups. Of the six dams obtained at each time point, three were used for histopathological analyses and three for reverse transcription-polymerase chain reaction (RT-PCR) analysis.

For the histopathological analysis, collected placentas were fixed in 10% neutral-buffered formalin, and 4-μm paraffin sections were stained with hematoxylin-eosin (HE). The sections were also subjected to the detection of fragmented DNA and immunohistochemical staining.

Detection of Fragmented DNA

Cells with fragmented DNA were detected by the terminal deoxynucleotidyltransferase-mediated dUTP end labeling (TUNEL) method, which was first proposed by Gavrieli [28] and is now widely used for the detection of apoptotic cells, using an apoptosis detection kit (Apop Tag; Intergen, Purchase, NY). In brief, multiple fragmented DNA 3′-OH ends on the section were labeled with digoxigenin-dUTP in the presence of terminal deoxynucleotidyl transferase (TdT). Peroxidase-conjugated anti-digoxigenin antibody was then reacted with the sections. The positive signals were visualized using a peroxidase-diaminobenzidine (DAB) reaction. The sections were then counterstained with methylgreen.

Immunohistochemical Staining

Immunohistochemical staining for cleaved caspase-3, topoisomerase IIα (TIIα), and p53 was carried out on paraffin sections. Cleaved caspase-3 is one of the key executioners of apoptosis and is responsible for the proteolytic cleavage of many key proteins to yield the apoptotic phenotype [29]. TIIα is a proliferation marker of rat and human tissues that is detected in the S to G2/M phase of the cell cycle [30]. Rabbit anticleaved caspase-3 polyclonal antibody (Cell Signaling Technology, Beverly, MA), mouse anti-TIIα monoclonal antibody (DAKO, Carpinteria, CA), and rabbit anti-p53 polyclonal antibody (Santa Cruz Biotechnology, Santa Cruz, CA) were used as primary antibodies. Sections were stained by the labeled streptavidin-biotin (LSAB) method with streptavidin (DAKO) for cleaved caspase-3 and TIIα, and by EnVision+ polymer reagent (DAKO) for p53. The positive signals were visualized with a peroxidase-DAB reaction and then the sections were counterstained with methylgreen.

Morphometry

To examine the incidence of apoptotic cell death, TUNEL-positive trophoblastic cells in the placental labyrinth zone were counted in three randomly chosen placentas from a dam. Three hundred cells were counted in randomly chosen fields of labyrinth zone in each placenta under a light microscope. For the assessment of proliferative activity, TIIα-positive trophoblastic cells were counted on the immunohistochemically stained sections and mitotic cells on the HE-stained sections in the same way. To examine p53 protein expression, p53-positive trophoblastic cells were also counted on the immunohistochemically stained sections. The apoptotic, mitotic, and TIIα- or p53-labeling indices (%) were expressed as the mean ± standard deviation (SD) for 3 dams, and statistical analysis was carried out with Student *t*-test.

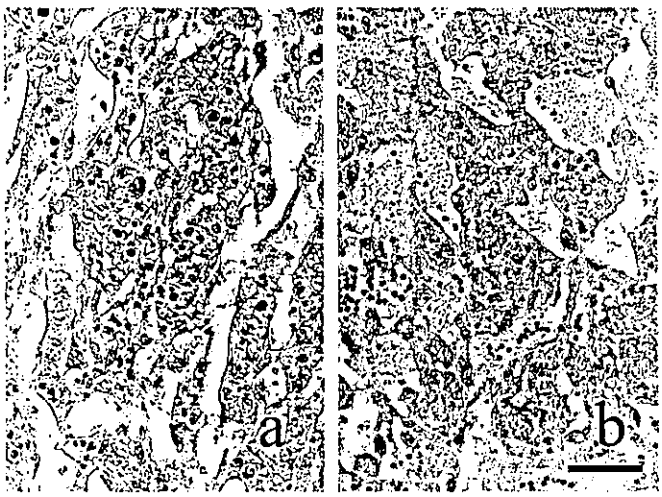

FIG. 1. Placenta of the Ara-C-treated (a) and control (b) rats at 6 h after the treatment. Many TUNEL-positive trophoblastic cells are seen in the labyrinth zone in a. TUNEL staining; bar = 55 μm.

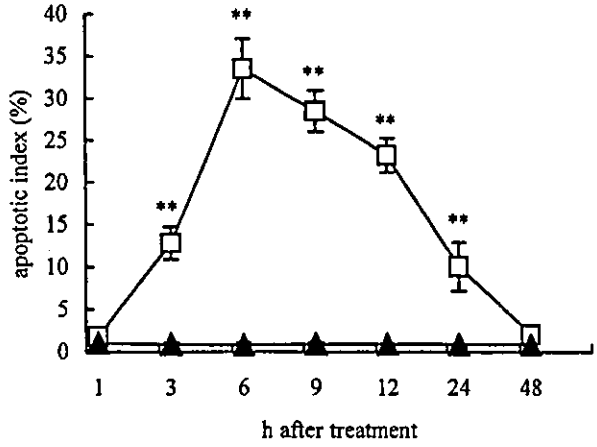

FIG. 2. Apoptotic index in the labyrinth zone. The number of apoptotic trophoblastic cells peaked at 6 h and returned to control levels at 48 h after the treatment. Data represent the mean ± SD (n = 3). **, $P < 0.01$; significantly different from controls. Open squares, Ara-C-treated group; closed triangles, control group.

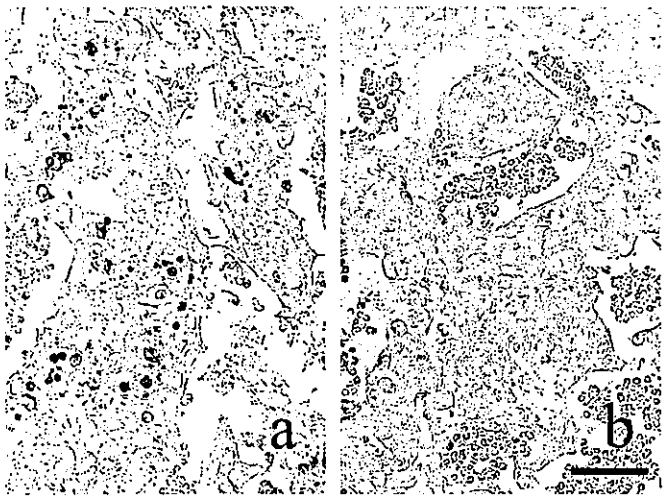

FIG. 3. Placenta of the Ara-C-treated (a) and control (b) rats at 6 h after the treatment. Many positive signals for cleaved caspase-3 are detected in the trophoblastic cells of the labyrinth zone in a. Immunostaining for cleaved caspase-3; bar = 40 μm.

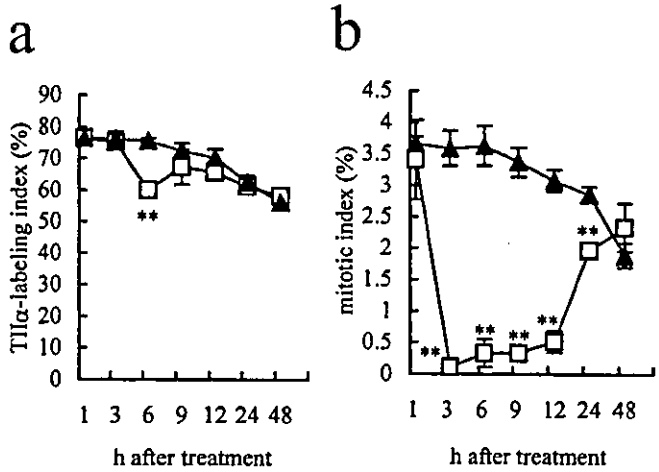

FIG. 5. TIIα-labeling (a) and mitotic (b) indices in the labyrinth zone. A significant decrease in the immunoreactivity for TIIα was detected at 6 h after the Ara-C-treatment. The number of mitotic figures was significantly suppressed from 3 to 24 h after the treatment. Data represent the mean ± SD (n = 3). **, $P < 0.01$; significantly different from controls. Open squares, Ara-C-treated group; closed triangles, control group.

RNA Extraction and Semiquantitative RT-PCR

The mRNA expression of p53 and three of its well-known target genes, *p21* [31], *cyclinG1* [32], and *fas* [33], was examined. Protein p21 is an inhibitor of cyclin-dependent kinases and induces cell-cycle arrest at the G1 phase [34]. CyclinG1 dephosphorylates mdm2, a negative regulator of p53, and modulates its function [35]. Fas is a type I membrane protein that belongs to the tumor necrosis factor receptor/nerve growth factor receptor family, and it induces apoptosis when it binds to fas ligand [36].

Three or four randomly chosen placentas from a dam were dissected to remove decidua and pooled. Then total RNA was extracted using Isogen (Nippon Gene Co. Ltd., Toyama, Japan). The reverse transcriptase reaction for synthesis of the first strand cDNA was carried out with 15 μg of sample in 60 μl of reaction mixture using oligo$(dT)_{12-18}$ primer and a SUPERSCRIPT Preamplification System (Invitrogen, Carlsbad, CA). PCR was performed with pairs of oligonucleotide primers corresponding to the cDNA sequences of the rat mRNA (Table 1). PCR was carried out with 1 μl of RT product in a 100-μl reaction mixture containing 50 pM of sense and antisense primer, 1.25 U of rTaq, 10× PCR buffer and dNTP mixture (Takara, Ohtsu, Japan). This was immediately followed by preheating at 94°C for 7 min, denaturation at 94°C for 1 min, annealing at 58.5°C for 1 min, and extension at 72°C for 1 min using a Takara PCR Thermal Cycler MP (Takara). Cycle numbers for different reactions are shown in Table 1. Optimal cycle numbers were determined in a preliminary experiment to ensure that the amplification of each gene was in the linear range and not during the plateau phase. PCR products were identified by electrophoresis on 2% agarose gels (Nippon Gene Co. Ltd.) followed by ethidium bromide (Invitrogen) staining. Fluorescent-gel imaging was carried out using an ultraviolet-CCD video system Fas-III (Toyobo, Tokyo, Japan). The results are shown relative to glyceraldehyde-3-phosphate dehydrogenase (GAPDH) expression. The relative band density is presented as the mean ± SD for three dams and statistical analysis was carried out using Student *t*-test.

RESULTS

Incidence of Apoptosis

From 3 h after the Ara-C treatment, the number of TUNEL-positive nuclei, which showed pyknosis on HE-stained sections, began to increase in trophoblastic cells of the placental labyrinth zone (Fig. 1). In our previous study, it was confirmed that the ultrastructural characteristics of these pyknotic cells were consistent with those of apoptotic

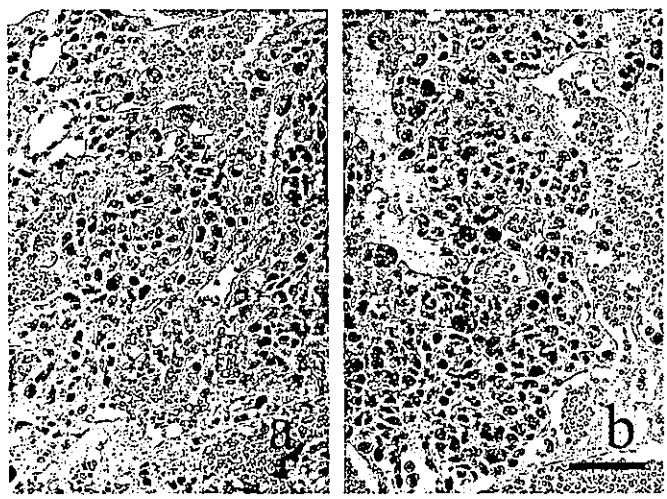

FIG. 4. Placenta of the Ara-C-treated (a) and control (b) rats at 6 h after the treatment. The number of TIIα-positive nuclei of trophoblastic cells is decreased in the labyrinth zone in a. Immunostaining for TIIα; bar = 55 μm.

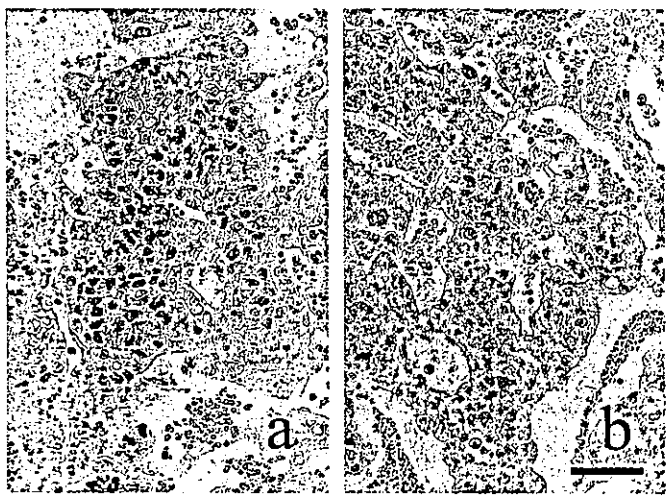

FIG. 6. Placenta of the Ara-C-treated (a) and control (b) rats at 3 h after the treatment. Many positive signals for p53 are detected in the nuclei of trophoblastic cells in the labyrinth zone in a. Immunostaining for p53; bar = 55 μm.

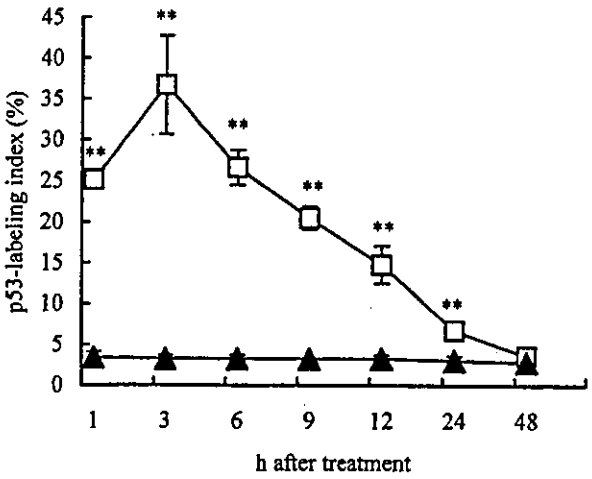

FIG. 7. The p53-labeling index in the labyrinth zone. The number of p53-positive nuclei of trophoblastic cells peaked at 3 h and returned to control levels at 48 h after the treatment. Data represent the mean ± SD (n = 3). **, $P < 0.01$; significantly different from controls. Open squares, Ara-C-treated group; closed triangles, control group.

cells [27]. The number peaked at 6 h after the treatment and returned to control levels at 48 h (Fig. 2). Only a few apoptotic cells were observed in the placental labyrinth zone in control dams throughout the experimental period (Figs. 1 and 2). In the placental basal zone of both the Ara-C-treated and control dams, only a few pyknotic cells were detected (data not shown).

At 6 h after the Ara-C-treatment, many positive signals for cleaved caspase-3 were detected in the trophoblastic cells of the placental labyrinth zone by immunohistochemistry (Fig. 3). On the other hand, only a few positive signals were observed in the placental labyrinth zone of control dams at 6 h after the treatment (Fig. 3).

Proliferative Activity

With the immunohistochemistry for TIIα, many positive signals were observed in the trophoblastic cells of the placental labyrinth zone in both the Ara-C-treated and control groups. A significant decrease in the immunoreactivity was detected at 6 h after the treatment (Figs. 4 and 5). The number of mitotic figures in the placental labyrinth zone decreased rapidly and reached a minimum at 3 h after the Ara-C treatment. The mitotic index was suppressed significantly until 24 h after the treatment, and then returned to control levels at 48 h (Fig. 5).

Expression of p53 Protein

In the placental labyrinth zone of the Ara-C-treated group, the number of p53-positive signals in the nuclei of trophoblastic cells began to increase from 1 h and peaked at 3 h after the treatment (Fig. 6). Then the number declined from 6 h and returned to control levels at 48 h after the treatment (Fig. 7). In the control group, only a few p53-positive signals were observed in the labyrinth zone throughout the experimental period (Figs. 6 and 7).

Expression of p53 and Its Transcriptional Target Genes mRNAs

The expression of *p53* mRNA changed little throughout the experimental period. The expression of *p21*, *cyclinG1*, and *fas* mRNAs significantly increased in the Ara-C-treated group. The expression of *p21*, *cyclinG1*, and *fas* mRNAs gradually increased from 3 h and peaked at around 9 h, then returned to control levels at 24 or 48 h after the treatment (Figs. 8 and 9).

DISCUSSION

As mentioned above, we previously demonstrated that the administration of Ara-C to pregnant rats caused significant decreases of placental weight and thickness of the labyrinth zone concomitant with increased apoptosis in the trophoblastic cells of the placental labyrinth zone [27]. In the present study, we detected a marked increase in the number of TUNEL-positive cells from 3 h to 24 h after the exposure to Ara-C. We also observed increased immunoreactivity for cleaved caspase-3. Caspase-3 is an effector of apoptosis thought to have a tissue- and stimulus-specific function [29]. We considered that caspase-3 would be an important executor of apoptosis also in placenta exposed to genotoxic stress. In addition, an analysis of TIIα-labeling and mitotic indices showed that proliferative activity was substantially suppressed in trophoblastic cells of the placental labyrinth zone. These results suggest that both increased cell death and suppressed cell proliferation result in the growth inhibition of the placenta observed in our previous report.

Several investigators recently demonstrated that, strictly speaking, the TUNEL technique is not specific for apoptosis and it also detects a small population of necrotic cells [37]. However, in our studies, TUNEL-positive trophoblastic cells were considered to be apoptotic ones judging from their electron microscopical features [27] and immunoreactivity for cleaved caspase-3.

Increased apoptosis is reported in human placenta complicated with intrauterine growth retardation or other abnormal pregnancies, and it is believed to be associated with placental dysfunction [6–10]. Trophoblastic cells in the placental labyrinth zone are a barrier to transport between maternal and fetal blood that actively facilitate the feto-maternal exchange of nutrients such as glucose, amino acids, fatty acids, and nucleosides [38]. Thus, a functional placental labyrinth zone would be indispensable for the

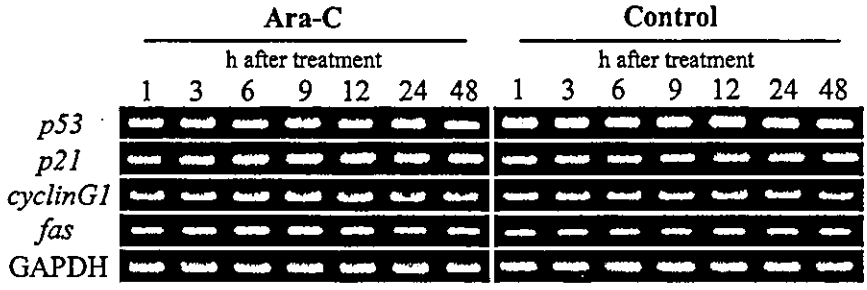

FIG. 8. Sequential changes in the mRNA expression of *p53* and its target genes. The expression of p53 target genes is enhanced after the Ara-C treatment. Agarose gel electrophoresis.

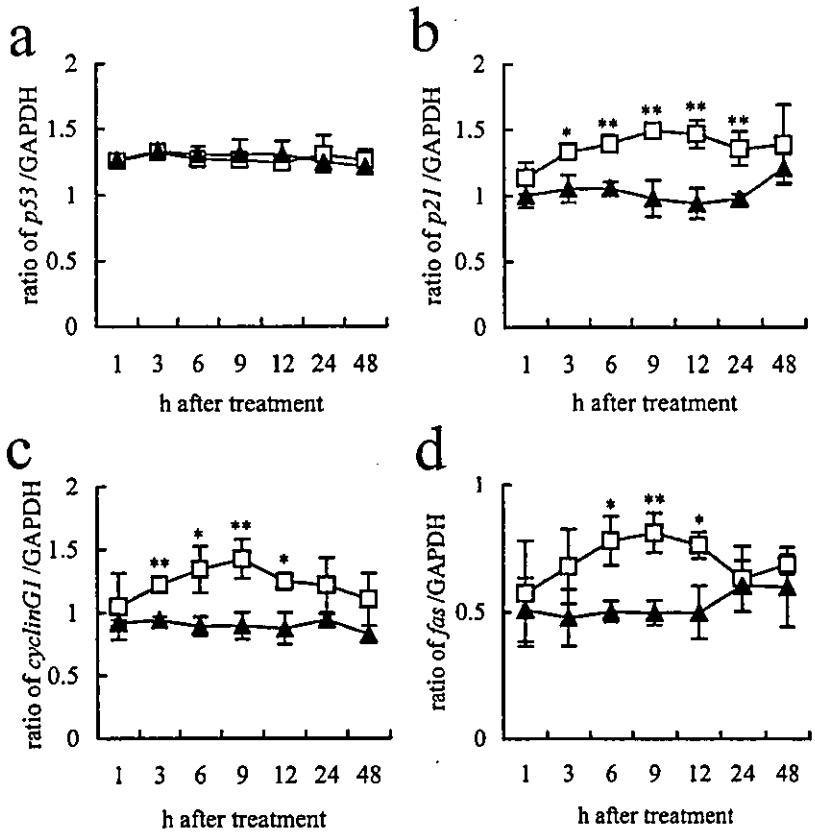

FIG. 9. Sequential changes in the expression of *p53* (a), *p21* (b), *cyclinG1* (c), and *fas* (d) mRNAs in the placenta exposed to Ara-C. Data represent the mean ± SD (n = 3). *, $P < 0.05$, **, $P < 0.01$; significantly different from controls. Open squares, Ara-C-treated group; closed triangles, control group.

growth, development, and well being of the fetus. In the present study, we demonstrated that Ara-C caused increased apoptotic cell death and impaired cell proliferation in the placental labyrinth zone. These toxic effects on trophoblastic cells would disrupt the function of the placental labyrinth zone, resulting in abnormal fetal development.

In the placenta, the expression of various genes that regulate apoptosis and proliferation, including p53, has been reported [39–42], and the death as well as growth of placental component cells is believed to be strictly controlled by these genes. In the present study, immunohistochemical examination revealed that a substantial elevation of p53 protein expression preceded Ara-C-induced changes in the apoptosis and proliferation of trophoblastic cells. In response to DNA damage, p53 protein is modified via phosphorylation or acetylation and becomes stabilized and activated. In a lot of cases, the function of p53 is mediated by those posttranscriptional mechanisms increasing the half-life and transcriptional activity of the protein [43, 44]. In our case, overexpression of *p53* mRNA was not detected in spite of the increase in the expression of p53 protein, and this suggests that p53 is regulated by such a posttranscriptional mechanism. On the other hand, the up-regulation of the p53 target genes mRNAs was observed following the increase in the expression of p53 protein, implying that p53 exerts its function by transactivation. Therefore, it is suggested that p53 and its transcriptional target genes are involved in the Ara-C-induced trophoblastic cell apoptosis and inhibition of cell proliferation in the placental labyrinth zone.

Ethylnitrosourea, a DNA alkylating teratogenic drug, was also reported to cause apoptosis and cell-cycle arrest with up-regulation of p53 protein in trophoblastic cells in the placental labyrinth zone [21]. In fetal central nervous system, targeted disruption of p53 critically suppressed apoptotic cell death induced by the administration of Ara-C [17] and ethylnitrosourea [45] to dams. The results of studies using Ara-C and ethylnitrosourea indicate that trophoblastic cells in the placental labyrinth zone are highly susceptible to genotoxic stimuli and p53 plays an important role in mediating the toxic effect of these stresses. Increased expression of p53 protein is also reported in human placenta complicated with fetal growth restriction [46]; thus, there is a possibility that stimuli such as hypoxia other than genotoxic stress cause placental disability in a p53-mediated way.

In addition to DNA damaging agents, endocrinological abnormality, inflammatory cytokines, and oxidative stress are demonstrated to induce placental apoptosis, and the distribution of the lesion is specific to the stimulus [5, 11, 12], suggesting that the pathways of increased placental apoptosis differ. Trophoblastic cells in the placental labyrinth zone actively proliferate and synthesize DNA [47], and this would have some relation to their sensitivity because Ara-C is cytotoxic to proliferating cells, especially in the DNA synthetic phase of the cell cycle [48]. However, the mechanism of the zone-dependent placental apoptosis under various pathological conditions is still obscure, and further study is needed to clarify this point.

In conclusion, the placenta is susceptible to genotoxic stress, including DNA damaging agents, which disrupt the regulation of trophoblastic cell death and proliferation. In addition, our findings suggest that p53 and its transcriptional target genes play an important role in the pathogenesis of Ara-C-induced placental toxicity. Probably, this induces placental growth inhibition and subsequent dysfunction of the placenta, which severely affects the development of the fetus, resulting in the induction of fetal growth restriction and other abnormal fetal development.

REFERENCES

1. Bauer MK, Harding JE, Bassett NS, Breier BH, Oliver MH, Gallaher BH, Evans PC, Woodall SM, Gluckman PD. Fetal growth and placental function. Mol Cell Endocrinol 1998; 140:115–120.
2. Smith SC, Baker PN, Symonds EM. Placental apoptosis in normal human pregnancy. Am J Obstet Gynecol 1997; 177:57–65.
3. Lea RG, Riley SC, Antipatis C, Hannah L, Ashworth CJ, Clark DA, Critchley HO. Cytokines and the regulation of apoptosis in reproductive tissues: a review. Am J Reprod Immunol 1999; 42:100–109.
4. Halperin R, Peller S, Rotschild M, Bukovsky I, Schneider D. Placental apoptosis in normal and abnormal pregnancies. Gynecol Obstet Invest 2000; 50:84–87.
5. Waddell BJ, Hisheh S, Dharmarajan AM, Burton PJ. Apoptosis in rat placenta is zone-dependent and stimulated by glucocorticoids. Biol Reprod 2000; 63:1913–1917.
6. Smith SC, Baker PN, Symonds EM. Increased placental apoptosis in intrauterine growth restriction. Am J Obstet Gynecol 1997; 177:1395–1401.
7. Smith SC, Baker PN. Placental apoptosis is increased in postterm pregnancies. Br J Obstet Gynaecol 1999; 106:861–862.
8. Axt R, Kordina AC, Meyberg R, Reitnauer K, Mink D, Schmidt W. Immunohistochemical evaluation of apoptosis in placentae from normal and intrauterine growth-restricted pregnancies. Clin Exp Obstet Gynecol 1999; 26:195–198.
9. Erel CT, Dane B, Calay Z, Kaleli S, Aydinli K. Apoptosis in the placenta of pregnancies complicated with IUGR. Int J Gynaecol Obstet 2001; 73:229–235.
10. Ishihara N, Matsuo H, Murakoshi H, Laoag-Fernandez JB, Samoto T, Maruo T. Increased apoptosis in the syncytiotrophoblast in human term placentas complicated by either preeclampsia or intrauterine growth retardation. Am J Obstet Gynecol 2002; 186:158–166.
11. Miller MJ, Voelker CA, Olister S, Thompson JH, Zhang XJ, Rivera D, Eloby-Childress S, Liu X, Clark DA, Pierce MR. Fetal growth retardation in rats may result from apoptosis: role of peroxynitrite. Free Radic Biol Med 1996; 21:619–629.
12. Ejima K, Koji T, Tsuruta D, Nanri H, Kashimura M, Ikeda M. Induction of apoptosis in placentas of pregnant mice exposed to lipopolysaccharides: possible involvement of Fas/Fas ligand system. Biol Reprod 2000; 62:178–185.
13. Chiba K, Ishikawa H, Rahman ME, Endo A. Neonatal mouse hip joint and hindlimb anomalies induced by prenatal exposure to Ara-C. Reprod Toxicol 1996; 10:215–219.
14. Vlahovic M, Bulic-Jakus F, Juric-Lekic G, Fucic A, Maric S, Serman D. Changes in the placenta and in the rat embryo caused by the demethylating agent 5-azacytidine. Int J Dev Biol 1999; 43:843–846.
15. Wang B, Ohyama H, Haginoya K, Odaka T, Yamada T, Hayata I. Prenatal radiation-induced limb defects mediated by Trp53-dependent apoptosis in mice. Radiat Res 2000; 154:673–679.
16. Katayama K, Ishigami N, Suzuki M, Ohtsuka R, Kiatipattanasakul W, Nakayama H, Doi K. Teratologic studies on rat perinates and offspring from dams treated with ethylnitrosourea (ENU). Exp Anim 2000; 49: 181–187.
17. D'Sa-Eipper C, Leonard JR, Putcha G, Zheng TS, Flavell RA, Rakic P, Kuida K, Roth KA. DNA damage-induced neural precursor cell apoptosis requires p53 and caspase 9 but neither Bax nor caspase 3. Development 2001; 128:137–146.
18. Katayama K, Ohtsuka R, Takai H, Nakayama H, Doi K. Expression of p53 and its transcriptional target genes mRNAs in the ethylnitrosourea-induced apoptosis and cell cycle arrest in the fetal central nervous system. Histol Histopathol 2002; 17:715–720.
19. Ueno M, Katayama K, Nakayama H, Doi K. Mechanisms of 5-azacytidine (5AzC)-induced toxicity in the rat foetal brain. Int J Exp Pathol 2002; 83:139–150.
20. Ko LJ, Prives C. p53: puzzle and paradigm. Genes Dev 1996; 10: 1054–1072.
21. Katayama K, Ueno M, Takai H, Ejiri N, Uetsuka K, Nakayama H, Doi K. Ethylnitrosourea induces apoptosis and growth arrest in the trophoblastic cells of rat placenta. Biol Reprod 2002; 67:431–435.
22. Wagner VM, Hill JS, Weaver D, Baehner RL. Congenital abnormalities in baby born to cytarabine treated mother. Lancet 1980; 2:98–99.
23. Schafer AI. Teratogenic effects of antileukemic chemotherapy. Arch Intern Med 1981; 141:514–515.
24. Volkenandt M, Buchner T, Hiddemann W, Van de Loo J. Acute leukaemia during pregnancy. Lancet 1987; 2:1521–1522.
25. Chaube S, Kreis W, Uchida K, Murphy ML. The teratogenic effect of 1-β-D-arabinofuranosylcytosine in the rat. Protection by deoxycytidine. Biochem Pharmacol 1968; 17:1213–1216.
26. Ritter EJ, Scott WJ, Wilson JG. Teratogenesis and inhibition of DNA synthesis induced in rat embryos by cytosine arabinoside. Teratology 1971; 4:7–13.
27. Yamauchi H, Katayama K, Yasoshima A, Uetsuka K, Nakayama H, Doi K. 1-β-D-Arabinofuranosylcytosine (Ara-C)-induced apoptosis in the rat fetal tissues and placenta. J Toxicol Pathol 2003; 16:223–229.
28. Gavrieli Y, Sherman Y, Ben-Sasson SA. Identification of programmed cell death in situ via specific labeling of nuclear DNA fragmentation. J Cell Biol 1992; 119:493–501.
29. Los M, Wesselborg S, Schulze-Osthoff K. The role of caspases in development, immunity, and apoptotic signal transduction: lessons from knockout mice. Immunity 1999; 10:629–639.
30. Woessner RD, Mattern MR, Mirabelli CK, Johnson RK, Drake FH. Proliferation- and cell cycle-dependent differences in expression of the 170 kilodalton and 180 kilodalton forms of topoisomerase II in NIH-3T3 cells. Cell Growth Differ 1991; 2:209–214.
31. el-Deiry WS, Tokino T, Velculescu VE, Levy DB, Parsons R, Trent JM, Lin D, Mercer WE, Kinzler KW, Vogelstein B. WAF1, a potential mediator of p53 tumor suppression. Cell 1993; 75:817–825.
32. Okamoto K, Beach D. Cyclin G is a transcriptional target of the p53 tumor suppressor protein. Embo J 1994; 13:4816–4822.
33. Muller M, Wilder S, Bannasch D, Israeli D, Lehlbach K, Li-Weber M, Friedman SL, Galle PR, Stremmel W, Oren M, Krammer PH. p53 activates the CD95 (APO-1/Fas) gene in response to DNA damage by anticancer drugs. J Exp Med 1998; 188:2033–2045.
34. Dulic V, Kaufmann WK, Wilson SJ, Tlsty TD, Lees E, Harper JW, Elledge SJ, Reed SI. p53-dependent inhibition of cyclin-dependent kinase activities in human fibroblasts during radiation-induced G1 arrest. Cell 1994; 76:1013–1023.
35. Okamoto K, Li H, Jensen MR, Zhang T, Taya Y, Thorgeirsson SS, Prives C. Cyclin G recruits PP2A to dephosphorylate Mdm2. Mol Cell 2002; 9:761–771.
36. Itoh N, Yonehara S, Ishii A, Yonehara M, Mizushima S, Sameshima M, Hase A, Seto Y, Nagata S. The polypeptide encoded by the cDNA for human cell surface antigen Fas can mediate apoptosis. Cell 1991; 66:233–243.
37. Levin S, Bucci TJ, Cohen SM, Fix AS, Hardisty JF, LeGrand EK, Maronpot RR, Trump BF. The nomenclature of cell death: recommendations of an ad hoc Committee of the Society of Toxicologic Pathologists. Toxicol Pathol 1999; 27:484–490.
38. Knipp GT, Audus KL, Soares MJ. Nutrient transport across the placenta. Adv Drug Deliv Rev 1999; 38:41–58.
39. Rees WD, Hay SM, Fontanier-Razzaq NC, Antipatis C, Harries DN. Expression of the growth arrest genes (GAS and GADD) changes during organogenesis in the rat fetus. J Nutr 1999; 129:1532–1536.
40. Levy R, Nelson DM. To be, or not to be, that is the question. Apoptosis in human trophoblast. Placenta 2000; 21:1–13.
41. Ishihara N, Matsuo H, Murakoshi H, Laoag-Fernandez J, Samoto T, Maruo T. Changes in proliferative potential, apoptosis and Bcl-2 protein expression in cytotrophoblasts and syncytiotrophoblast in human placenta over the course of pregnancy. Endocr J 2000; 47:317–327.
42. Ka H, Hunt JS. Temporal and spatial patterns of expression of inhibitors of apoptosis in human placentas. Am J Pathol 2003; 163:413–422.
43. Lakin ND, Jackson SP. Regulation of p53 in response to DNA damage. Oncogene 1999; 18:7644–7655.
44. Brooks CL, Gu W. Ubiquitination, phosphorylation and acetylation: the molecular basis for p53 regulation. Curr Opin Cell Biol 2003; 15: 164–171.
45. Leonard JR, D'Sa C, Klocke BJ, Roth KA. Neural precursor cell apoptosis and glial tumorigenesis following transplacental ethyl-nitrosourea exposure. Oncogene 2001; 20:8281–8286.
46. Levy R, Smith SD, Yusuf K, Huettner PC, Kraus FT, Sadovsky Y, Nelson DM. Trophoblast apoptosis from pregnancies complicated by fetal growth restriction is associated with enhanced p53 expression. Am J Obstet Gynecol 2002; 186:1056–1061.
47. Peel S, Bulmer D. Proliferation and differentiation of trophoblast in the establishment of the rat chorio-allantoic placenta. J Anat 1977; 124:675–687.
48. Grant S. Ara-C: cellular and molecular pharmacology. Adv Cancer Res 1998; 72:197–233.

Available online at www.sciencedirect.com

SCIENCE DIRECT

Neurotoxicology and Teratology 26 (2004) 579–586

NEUROTOXICOLOGY AND TERATOLOGY

www.elsevier.com/locate/neutera

Involvement of p53 in 1-β-D-arabinofuranosylcytosine-induced rat fetal brain lesions

Hirofumi Yamauchi*, Kei-ichi Katayama, Masaki Ueno, Koji Uetsuka, Hiroyuki Nakayama, Kunio Doi

Department of Veterinary Pathology, Graduate School of Agricultural and Life Sciences, The University of Tokyo, 1-1-1 Yayoi, Bunkyo, 113-8657 Tokyo, Japan

Received 22 January 2004; received in revised form 26 March 2004; accepted 26 March 2004
Available online 18 May 2004

Abstract

1-β-D-Arabinofuranosylcytosine (Ara-C), a cytidine analogue cytotoxic to proliferating cells, has a teratogenic effect in the brain of experimental animals and causes neural cell apoptosis in vitro and in vivo. In the present study, pregnant rats were injected with Ara-C on Day 13 of gestation and the fetal brain was collected from 1 to 48 h after treatment. Histopathological examinations revealed marked induction of apoptotic cell death and decrease of mitosis in neuroepithelial cells in the brain of Ara-C-treated fetus, and these changes were most prominent from 9 to 12 h. Expression of p53 protein, which mediates apoptosis and cell cycle arrest after DNA damage, was elevated remarkably and peaked at 3 h. *p21*, a cyclin-dependent kinase inhibitor responsible for p53-mediated cell cycle arrest, showed intense overexpression in protein and mRNA levels following the increase of p53 protein. The mRNA expressions of other p53 transcriptional target genes, *bax*, *cyclinG1*, and *fas*, also significantly increased and peaked at around 9 h. In conclusion, prenatal treatment of Ara-C is thought to induce apoptosis and inhibition of cell proliferation mediated by *p53* and its target genes in the fetal brain.

Keywords: Apoptosis; Ara-C; Fetus; p53; Rat; Central nervous system

1. Introduction

1-β-D-Arabinofuranosylcytosine (Ara-C), a cytidine analogue, inhibits DNA synthesis and is cytotoxic to proliferating cells especially in the DNA synthetic phase of the cell cycle [11]. Therefore, it has been used as one of the most effective agents in the clinical treatment for myelogenous leukemia [4] and other hematologic malignancies. On the other hand, prenatal treatment of Ara-C has a teratogenic effect and causes malformations of the brain such as encephalocele, hydrocephalus, and microcephaly in rats [1,5,22,23]. We previously reported that an injection of Ara-C into pregnant rats induced increased apoptosis in the brain and other organs of fetuses, which would be related with the teratogenicity of Ara-C [26].

The *p53* tumor suppressor gene is involved in the regulation of apoptosis and cell cycle arrest after DNA damage, thereby preventing the propagation of damaged cells in a number of different paradigms [15]. p21, a downstream target of p53, is an inhibitor of cyclin-dependent kinases and responsible for the cell cycle arrest in cells sustaining DNA damage [7].

Neural cells in various culture models develop apoptosis by the treatment of Ara-C, and p53 plays the key role in these responses [9,10,27]. It is also demonstrated that transplacental exposure of Ara-C failed to induce neural precursor cell apoptosis in the fetal telencephalon of *p53*-deficient mouse [6]. However, there are only a few reports regarding the incidence of apoptosis in the fetal brain exposed to Ara-C in vivo, and little is known about the expressional or functional patterns of *p53* and other related genes that would be essential for the cellular response to the Ara-C treatment.

The aim of the present study is to explore the more detailed process of Ara-C-induced cytotoxic effects in the developing fetal brain and to reveal its mechanisms in relation to *p53*. For the purpose, we examined the sequential histopathological changes in the fetal brain obtained from pregnant rats treated with Ara-C on Day 13 of gestation (GD13). Moreover, we investigated the

* Corresponding author. Tel./fax: +81-3-5841-8185.
E-mail address: yamauchi-h@umin.ac.jp (H. Yamauchi).

0892-0362/$ – see front matter © 2004 Elsevier Inc. All rights reserved.
doi:10.1016/j.ntt.2004.03.010

temporal expression patterns of p53 and p21 protein by immunohistochemistry and of *p53* and its target genes mRNAs by reverse transcription and polymerase chain reaction (RT-PCR).

2. Methods

2.1. Animals and chemicals

Pregnant Slc:Wistar rats (plug day: Day 0 of gestation) were obtained from Japan SLC, Shizuoka, Japan. They were kept under controlled conditions (temperature, 23 ± 2 °C; relative humidity, 55 ± 5%) using an isolator caging system (Niki Shoji, Tokyo) and were fed commercial pellets (MF, Oriental Yeast, Tokyo, Japan) and water ad libitum. Ara-C (Sigma, St. Louis, MO) was dissolved in phosphate-buffered saline (PBS). The protocol of the present study has been approved by the Animal Care and Use Committee of Graduate School of Agricultural and Life Sciences, The University of Tokyo.

2.2. Treatments

Pregnant rats were injected intraperitoneally with 250 mg/kg of Ara-C on GD 13. At 1, 3, 6, 9, 12, 24, and 48 h after treatment, six dams each were exsanguinated by heart puncture under ether anesthesia, and the fetuses were collected by Caesarian section. As controls, six pregnant rats were injected intraperitoneally with PBS on GD13 and sacrificed at the same time point as Ara-C-treated groups. Of the six dams obtained at each time point, three were used for histopathological and immunohistochemical analysis and three for RT-PCR analysis.

2.3. Histopathology and immunohistochemistry

Collected fetuses were fixed in 10% neutral-buffered formalin. For histopathological examination, 4-μm paraffin sections were stained with hematoxylin and eosin (HE).

For immunohistochemical examination, paraffin sections (4 μm) were deparaffinized and immersed in 10 mM citrate buffer, pH 6.0, and heated for 15 min at 121 °C by autoclave. After washing in Tris-buffered saline (TBS), the sections were placed in 0.3% H_2O_2-containing methanol for 30 min to inactivate endogenous peroxidase. Then the sections were incubated in skimmed milk for 40 min at 37 °C to reduce nonspecific staining and successively incubated in the rabbit anti-p53 polyclonal antibody (Santa Cruz Biotechnology, Santa Cruz, CA) or mouse anti-p21 monoclonal antibody (PharMingen, San Diego, CA) overnight at 4 °C and then in EnVision+polymer reagent (Dako, Carpinteria, CA) for 30 min at room temperature. These sections were washed in TBS for 15 min after each step. The positive signals were visualized using a peroxidase–diaminobenzidine reaction and then the sections were counterstained with methylgreen.

2.4. Morphometry

Apoptotic and mitotic neuroepithelial cells in the ventricular zone of the fetal telencephalic wall were counted in two randomly chosen fetuses from a dam on the HE-stained sections under light microscope. Five hundred cells were counted in each fetus. p53- or p21-positive surviving neuroepithelial cells were also counted in the same way on the immunohistochemically stained sections under light microscope. The apoptotic, mitotic, and p53- or p21-labeling indices (%) were expressed as the mean ± S.D. for three dams, and statistical analysis was carried out with Student's *t* test.

2.5. RNA extraction and semiquantitative RT-PCR

Six fetal telencephalon from a dam were pooled and total RNA was extracted using Isogen (Nippon Gene, Toyama, Japan). The reverse transcriptase reaction for synthesis of the first strand cDNA was carried out with 15 μg of sample in 60 μl of reaction mixture using oligo$(dT)_{12-18}$ primer and a Superscript Preamplification System (Invitrogen, Carlsbad, CA). Polymerase chain reaction was performed with pairs of oligonucleotide primers corresponding to the cDNA sequences of rat mRNA (Table 1). PCR was carried out with 1 μl of RT product in a 100-μl reaction mixture containing 50 pM of sense and antisense primer, 1.25 U rTaq, 10 × PCR buffer, and dNTP mixture (Takara, Ohtsu, Japan). This was immediately followed by preheating at 94 °C for 7 min, denaturation at 94 °C for 1 min, annealing at 58.5 °C for

Table 1
Primer sequences and cycle numbers

Gene	Sense primer	Antisense primer	Cycle number
p53	ATATGAGCATCGAGCTCCCTCT	CACAACTGCACAGGGCATGT	25
p21	AAGTATGCCGTCGTCTGTTCG	GGCACTTCAGGGCTTTCTCTT	28
bax	TTCATCCAGGATCGAGCAGAG	TGAGGACTCCAGCCACAAAGAT	25
cyclinG1	GTGTCGGACTGAGCTGCTTTT	TTGGGAGGTGGGTTATCCTGT	24
fas	AAGAGGAGCGTTCGTGAAACC	GATCAGCAGCCAAAGGAGCTTA	30
GAPDH	GCTTCACCACCTTCTTGATGTC	GAGTATGTCGTGGAGTCTACTG	20

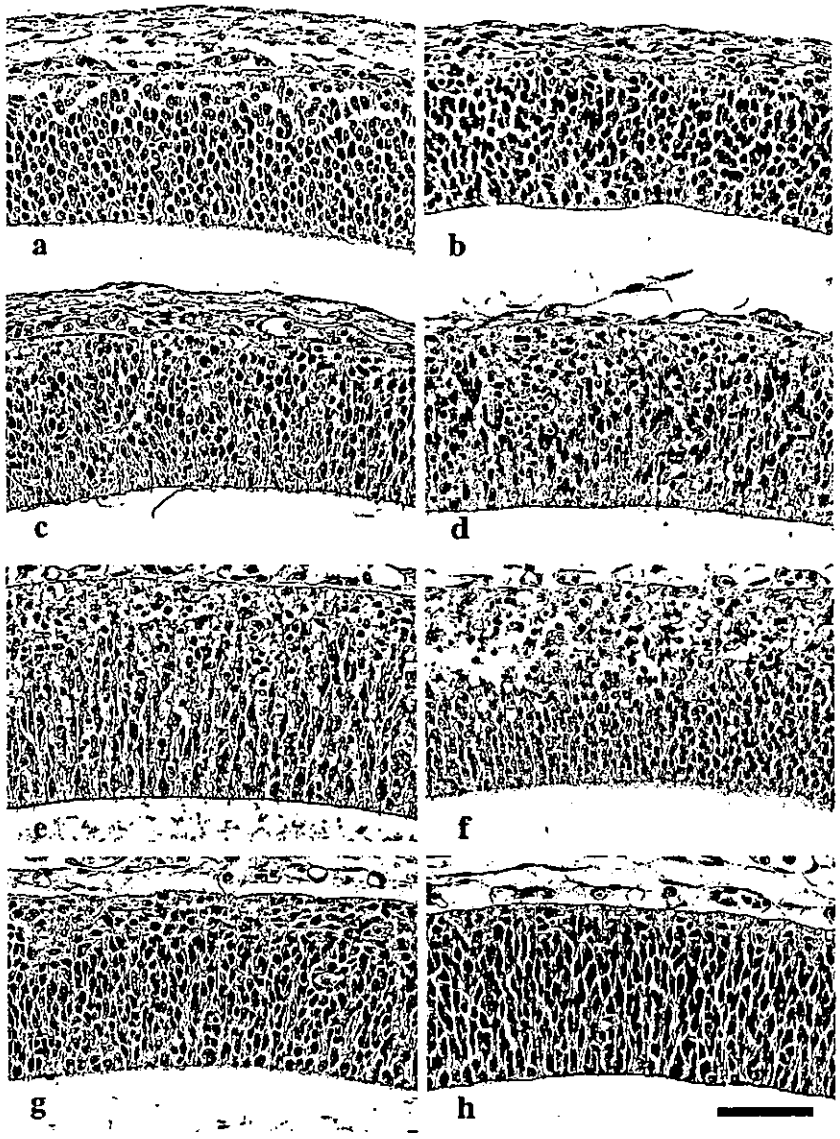

Fig. 1. Histological appearances of the telencephalic wall of the Ara-C-treated group at 1 (a), 3 (b), 6 (c), 9 (d), 12 (e), 24 (f), and 48 h (g) and of the control group at 9 h after treatment (h). Apoptotic cells were found from 3 h. The number of apoptotic cells peaked at 9 h, then gradually decreased and returned to the control level at 48 h. The number of mitotic cells decreased from 3 h and few mitotic cells were observed from 9 to 12 h. Then mitotic index began to recover from 24 h and reached the control level at 48 h. HE; Bar = 60 μm.

1 min, and extension at 72 °C for 1 min using Takara PCR Thermal Cycler MP (Takara). Cycle numbers for different PCR reactions are shown in Table 1. Optimal cycle numbers were determined by the preliminary experiment to ensure that the amplification of each gene was in the linear range and not during the plateau phase. PCR products were identified by electrophoresis on 2% agarose gels (Nippon Gene) followed by ethidium bromide (Invitrogen) staining. Fluorescent gel imaging was carried out using a UV-CCD video system Fas-III (Toyobo, Tokyo, Japan). The results are shown as a relative ratio to glyceraldehyde-3-phosphate dehydrogenase (GAPDH) expression. The relative band density is presented as the mean ± S.D. for three dams and statistical analysis was carried out using Student's *t* test.

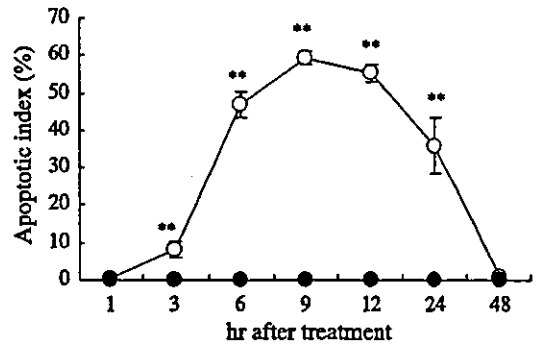

Fig. 2. Apoptotic index in the telencephalic wall of rat fetuses exposed to Ara-C on GD13. Data represent the mean ± S.D. ($n = 3$). $^{**}P < 0.01$; significantly different from controls. Open circles, Ara-C-treated group; closed circles, control group.

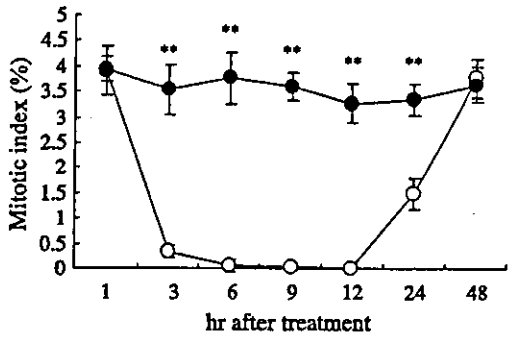

Fig. 3. Mitotic index in the telencephalic wall of rat fetuses exposed to Ara-C on GD13. Data represent the mean ± S.D. ($n=3$). $^{**}P<0.01$; significantly different from controls. Open circles, Ara-C-treated group; closed circles, control group.

3. Results

3.1. Histopathology

After transplacental exposure of Ara-C, the number of pyknotic neuroepithelial cells, which were shown to be apoptotic ones in our previous study [26], significantly increased in the ventricular zone of the fetal brain. The number began to increase from 3 h and peaked from 9 to 12 h after treatment. It declined from 24 h and nearly returned to the control level at 48 h. Few apoptotic cells were observed in the fetal brain from control dams throughout the experimental period (Figs. 1 and 2).

In the Ara-C-treated group, the number of mitotic figures of neuroepithelial cells in the ventricular zone began to

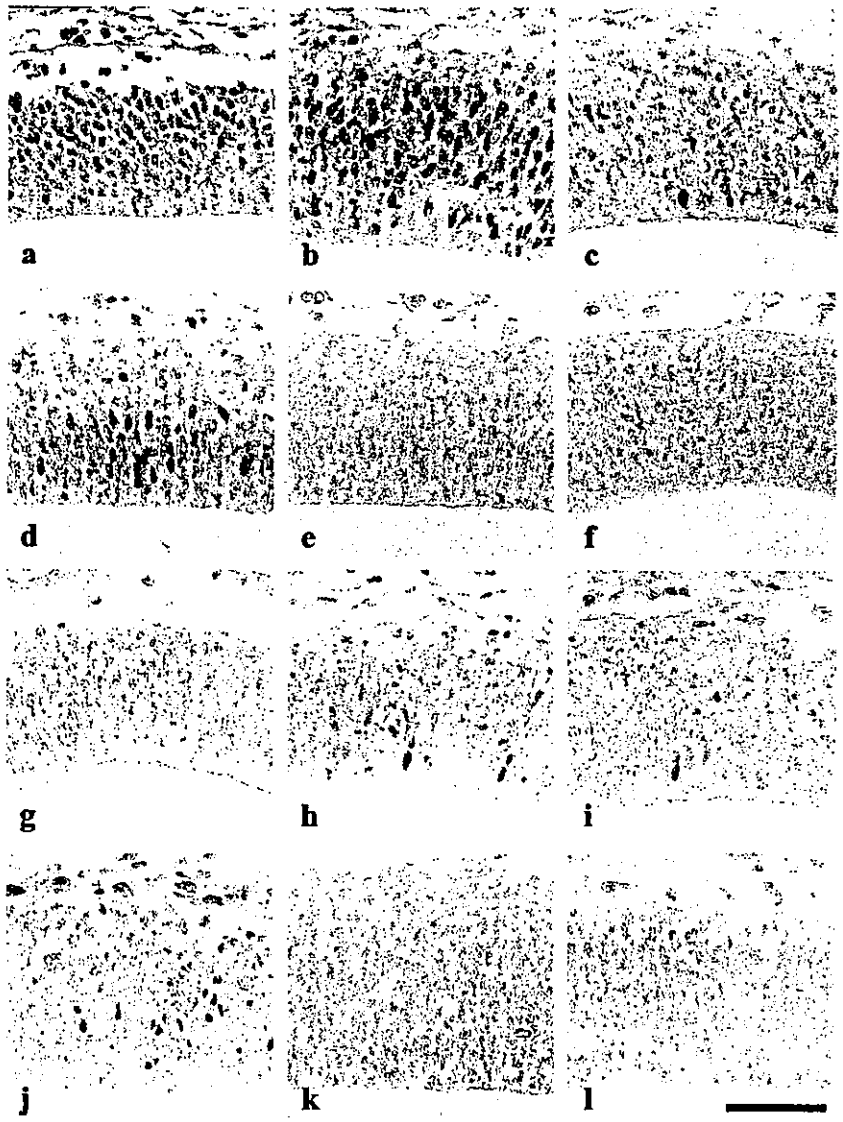

Fig. 4. Immunostaining for p53 (a–f) and p21 (g–l) in the telencephalic wall of rat fetuses. The number of p53-positive cells began to increase from 1 h (a) and reached the peak at 3 h after treatment (b). Then the number declined (c; 9 h) but increased again at 24 h (d). Finally, the number decreased and returned to the control level at 48 h (e). The number of p21-positive cells hardly changed until 3 h (g) and then abruptly peaked at 6 h (h). Subsequently, the number declined (i; 9 h) but again increased at 24 h (j). Finally, the number decreased and returned to the control level at 48 h (k). In the control fetuses, only a few p53- and p21-positive signals were observed (f and l). Bar = 60 μm.

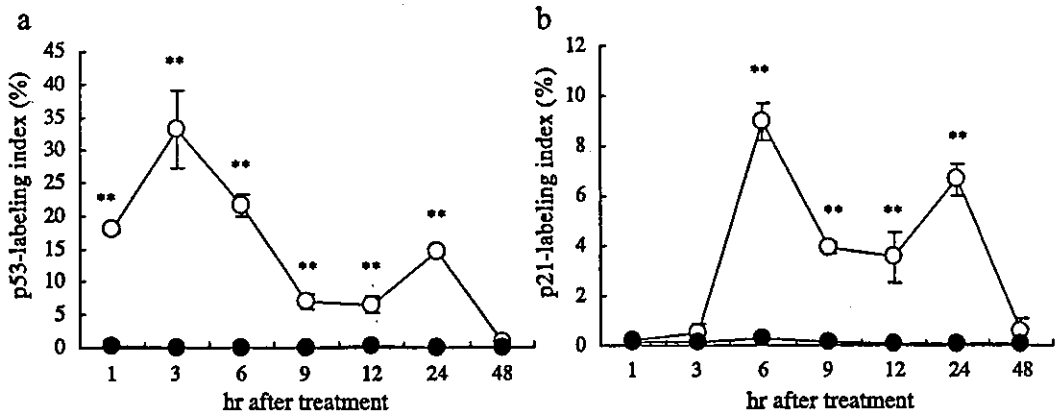

Fig. 5. p53 (a)- and p21-labeling index (b) in the telencephalic wall of rat fetuses exposed to Ara-C on GD13. Data represent the mean ± S.D. ($n=3$). ** $P<0.01$; significantly different from controls. Open circles, Ara-C-treated group; closed circles, control group.

decrease markedly from 3 h and few mitotic cells were observed from 9 to 12 h. Then the number began to recover from 24 h and reached the control level at 48 h. Mitotic index hardly changed in the control group throughout the experimental period (Figs. 1 and 3).

3.2. Immunohistochemistry

In the ventricular zone of the Ara-C-treated fetuses, the number of p53-positive signals in the nuclei of neuroepithelial cells increased from 1 h and peaked at 3 h after treatment. Then the number declined from 6 to 12 h but increased again at 24 h. Finally, the number decreased and returned to the control level at 48 h (Figs. 4a–e and 5a).

The number of p21-positive signals in the nuclei of neuroepithelial cells increased and reached the peak abruptly at 6 h. Then the number declined from 9 to 12 h and increased again at 24 h. Finally, the number decreased and returned to the control level at 48 h (Figs. 4g–k and 5b).

In the control fetuses, only a few p53- and p21-positive signals were observed in the nuclei of neuroepithelial cells throughout the experimental period (Figs. 4f, l, and 5).

3.3. Semiquantitative RT-PCR

The expressions of *p53* mRNA did not increase significantly throughout the experimental period. The expression of *p21*, *bax*, *cyclinG1*, and *fas* mRNAs significantly increased in the Ara-C-treated group. The expression of *p21* mRNA increased prominently from 3 to 24 h, and those of *bax*, *cyclinG1*, and *fas* mRNAs also increased and peaked at around 9 h after treatment (Figs. 6 and 7).

4. Discussion

p53 is activated by DNA-damaging agents or mitotic inhibitors [15]. It transactivates a series of genes including *p21* [8], *bax* [24], *cyclinG1* [20], and *fas* [19]. p21 is an inhibitor of cyclin-dependent kinases and it induces cell cycle arrest at G1 phase [7]. Bax is a proapoptotic member of the bcl-2 family. Increased bax/bcl-2 ratio enforces dimerization of *bax* and finally induces apoptosis [12]. CyclinG1 dephosphorylates mdm2, a negative regulator of p53, and modulates its function [21]. Fas is a type I membrane protein that belongs to tumor necrosis factor receptor/nerve growth factor receptor family [13] and it induces apoptosis when it binds to *fas* ligand.

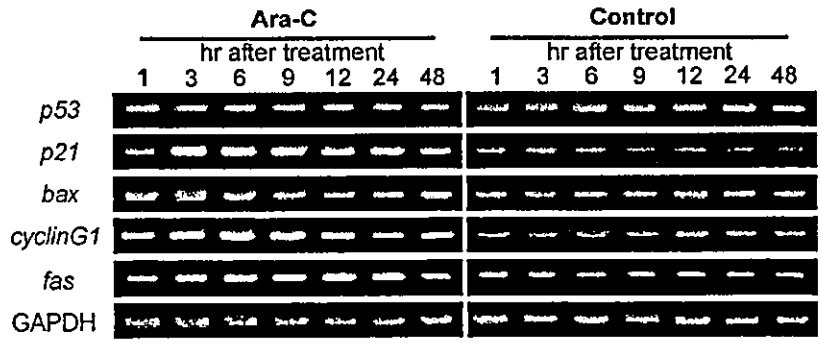

Fig. 6. Sequential changes of mRNA expression of p53 and its target genes. Agarose gel electrophoresis. Expressions of p53 target genes are elevated after Ara-C treatment.

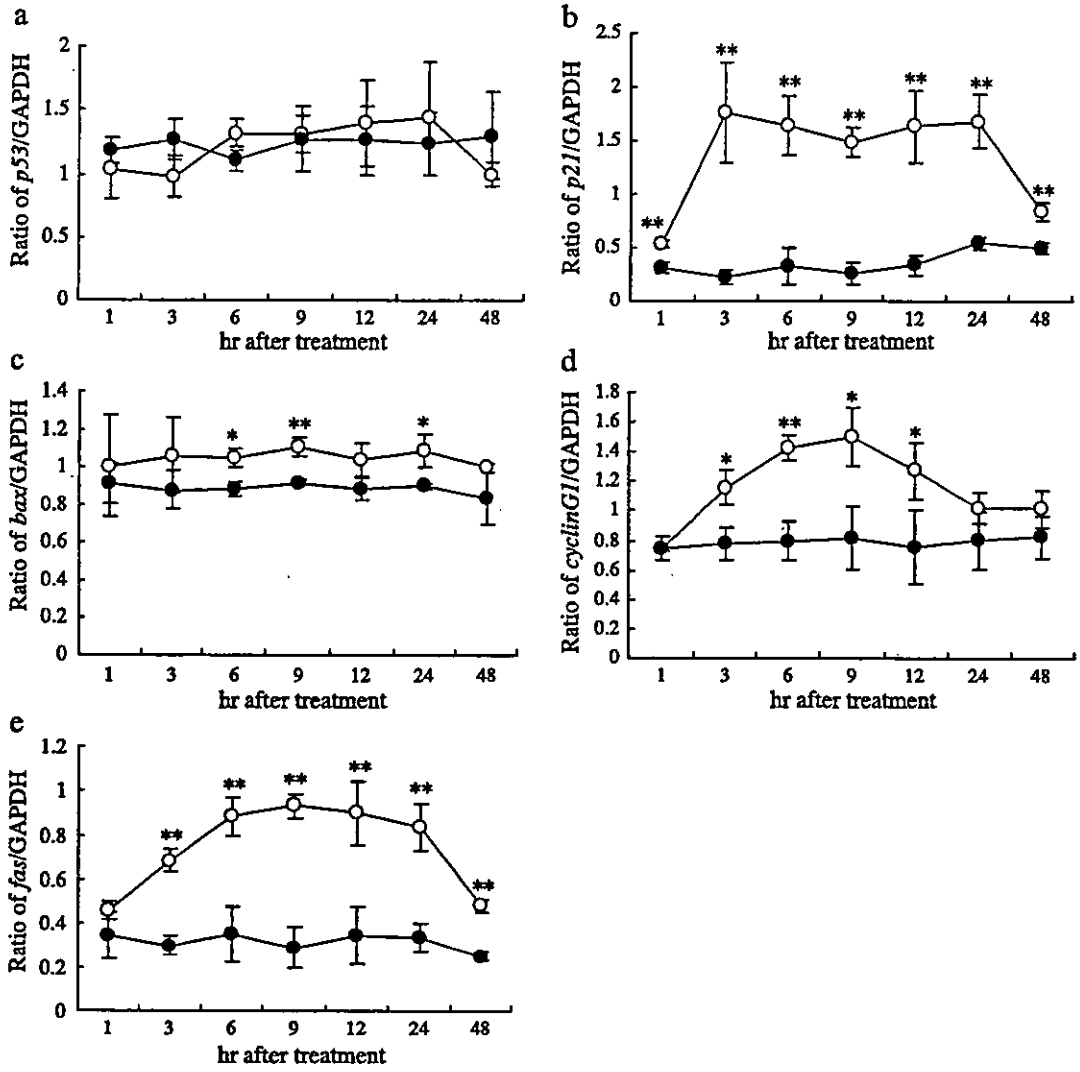

Fig. 7. Sequential changes of mRNA expression of *p53* (a), *p21* (b), *bax* (c), *cyclinG1* (d), and *fas* (e) in the brain of rat fetuses exposed to Ara-C on GD13. Data represent the mean ± S.D. ($n = 3$). * $P < 0.05$, ** $P < 0.01$; significantly different from controls. Open circles, Ara-C-treated group; closed circles, control group.

In the present study, the incidence of apoptosis in neuroepithelial cells of the fetal brain increased markedly whereas the number of mitotic cells decreased prominently after treatment with Ara-C. In addition, incorporation of 5-bromo-2′-deoxyuridine (BrdU) into neuroepithelial cell nuclei remarkably decreased after Ara-C treatment (data not shown). Immunohistochemical analysis revealed that the substantial increase of p53 protein expression preceded these histological changes. RT-PCR analysis showed that the expression of *p21* mRNA, which elevated most prominently among p53 target genes examined, began to increase markedly from 3 h after treatment when p53 protein level reached the peak. Subsequently, the expression of p21 protein increased and reached the maximal value at 6 h. The expressions of p53 and p21 protein increased again at 24 h and their expression patterns were well coincided with each other. The expression of other p53 target genes mRNAs significantly increased and peaked at around 9 h following the elevation of p53 protein. These findings suggest that accumulation of p53 protein transactivated its target genes including *p21* in the Ara-C-treated fetal brain. Since the mitotic index was suppressed during overexpression of p21, it is likely that p21 plays an important role in the induction of cell cycle arrest also in the present study. Neural precursor cells in the fetal telencephalon of *p53*-deficient mice did not develop apoptosis by the transplacental exposure of Ara-C [6], indicating that p53 is essential in Ara-C-induced apoptosis in vivo.

Our data suggest that transplacental exposure of Ara-C caused an induction of apoptosis and an inhibition of cell proliferation mediated by p53 and its transcriptional target genes in the fetal brain. On the other hand, though p21 is known to induce G1 arrest [7], it is not possible to confirm in which phase neuroepithelial cell cycle was arrested or retarded in our experiment, and further studies are needed to clarify this point.

In response to DNA damage, p53 protein is phosphorylated and becomes stabilized against disruption by the interaction with its negative regulator, mdm2. In a lot of cases, functional activation of p53 is mediated by the posttranscriptional mechanism increasing the half-life of the protein [16]. In our case, overexpression of *p53* mRNA was not detected in spite of the increase in p53 protein level, and this suggests that p53 is regulated by such a protein stabilization mechanism. In addition, immunohistochemical staining revealed that increased expression of p53 protein is localized in nuclei of neuroepithelial cells in the present study. This is consistent with the fact that p53 is accumulated and binds DNA in the nucleus of the damaged cell to exert its function [15].

Other DNA damaging teratogenic drugs, such as ethylnitrosourea and 5-azacytidine, also caused apoptosis and cell cycle arrest in the fetal brain with up-regulation and activation of p53 protein [14,25]. Besides chemicals, radiation induced apoptosis in the rat fetal brain in a *p53*-dependent manner [2], and brain anomalies were detected after birth [18]. These findings suggest that neural cells in the fetal brain are susceptible to DNA damaging stimuli, easily develop apoptosis and cell cycle arrest in a p53-dependent way, and a consequent decrease of neural cell population induced by excess cell death and suppressed cell proliferation may contribute to the formation of brain anomalies.

In the present study, secondary peaks were observed in the expression patterns of p53 and p21 protein at 24 h after treatment. Although further studies are needed to clarify its meaning, there are two possible explanations for this finding. First, neuroepithelial cells in the telencephalic ventricular zone are not composed of homogeneous cells; thus, reactions to Ara-C treatment would be different among those cells. In the stage of brain development, neuroepithelial cells move in the ventricular zone following a particular pattern [17]. In the process of their cell cycle, the nuclei of the neuroepithelial cells descend to the ventricular inner surface to undergo mitosis and subsequently return to the outer zone again. After that, some daughter cells move to cortical plate to differentiate into neuroblasts and others maintain their function as neuroepithelial cells and continue cell cycle in the ventricular zone. Thus, it is possible that protein expression patterns after Ara-C exposure were not the same in these cells even if they incorporate the drug at the same time, thereby resulting in the two separate peaks in the expression of p53 and p21 protein. Second, maternal and placental toxicity of Ara-C would affect the fetal tissues including brain. Prenatal treatment of Ara-C induced apoptosis in various fetal tissues such as hematopoietic progenitor cells and in placental trophoblasts [26]. Excess cell death in fetal tissues and placenta would impair the sustenance of brain development and indirectly increase p53 protein and its targets. Indeed, it is demonstrated that hypoxia caused p53 protein accumulation and overexpression of its downstream targets in cultured neuron [3].

In conclusion, our data suggest that transplacental exposure of Ara-C caused an induction of neuroepithelial cell apoptosis and an inhibition of cell proliferation through the mechanisms mediated by p53 and its transcriptional target genes in the fetal brain.

References

[1] B.P. Adlard, J. Dobbing, J. Sands, A comparison of the effects of cytosine arabinoside and adenine arabinoside on some aspects of brain growth and development in the rat, Br J Pharmacol 54 (1975) 33–39.

[2] S. Bolaris, E. Bozas, A. Benekou, H. Philippidis, F. Stylianopoulou, In utero radiation-induced apoptosis and p53 gene expression in the developing rat brain, Int J Radiat Biol 77 (2001) 71–81.

[3] C. Bossenmeyer-Pourie, V. Lievre, S. Grojean, V. Koziel, T. Pillot, J.L. Daval, Sequential expression patterns of apoptosis- and cell cycle-related proteins in neuronal response to severe or mild transient hypoxia, Neuroscience 114 (2002) 869–882.

[4] R.L. Capizzi, Curative chemotherapy for acute myeloid leukemia: the development of high-dose ara-C from the laboratory to bedside, Invest New Drugs 14 (1996) 249–256.

[5] S. Chaube, W. Kreis, K. Uchida, M.L. Murphy, The teratogenic effect of 1-β-D-arabinofuranosylcytosine in the rat. Protection by deoxycytidine, Biochem Pharmacol 17 (1968) 1213–1216.

[6] C. D'Sa-Eipper, J.R. Leonard, G. Putcha, T.S. Zheng, R.A. Flavell, P. Rakic, K. Kuida, K.A. Roth, DNA damage-induced neural precursor cell apoptosis requires p53 and caspase 9 but neither Bax nor caspase 3, Development 128 (2001) 137–146.

[7] V. Dulic, W.K. Kaufmann, S.J. Wilson, T.D. Tlsty, E. Lees, J.W. Harper, S.J. Elledge, S.I. Reed, p53-dependent inhibition of cyclin-dependent kinase activities in human fibroblasts during radiation-induced G1 arrest, Cell 76 (1994) 1013–1023.

[8] W.S. el-Deiry, T. Tokino, V.E. Velculescu, D.B. Levy, R. Parsons, J.M. Trent, D. Lin, W.E. Mercer, K.W. Kinzler, B. Vogelstein, WAF1, a potential mediator of p53 tumor suppression, Cell 75 (1993) 817–825.

[9] Y. Enokido, T. Araki, S. Aizawa, H. Hatanaka, p53 involves cytosine arabinoside-induced apoptosis in cultured cerebellar granule neurons, Neurosci Lett 203 (1996) 1–4.

[10] H.M. Geller, K.Y. Cheng, N.K. Goldsmith, A.A. Romero, A.L. Zhang, E.J. Morris, L. Grandison, Oxidative stress mediates neuronal DNA damage and apoptosis in response to cytosine arabinoside, J Neurochem 78 (2001) 265–275.

[11] S. Grant, Ara-C: cellular and molecular pharmacology, Adv Cancer Res 72 (1998) 197–233.

[12] A. Gross, J. Jockel, M.C. Wei, S.J. Korsmeyer, Enforced dimerization of BAX results in its translocation, mitochondrial dysfunction and apoptosis, EMBO J 17 (1998) 3878–3885.

[13] N. Itoh, S. Yonehara, A. Ishii, M. Yonehara, S. Mizushima, M. Sameshima, A. Hase, Y. Seto, S. Nagata, The polypeptide encoded by the cDNA for human cell surface antigen Fas can mediate apoptosis, Cell 66 (1991) 233–243.

[14] K. Katayama, R. Ohtsuka, H. Takai, H. Nakayama, K. Doi, Expression of p53 and its transcriptional target genes mRNAs in the ethylnitrosourea-induced apoptosis and cell cycle arrest in the fetal central nervous system, Histol Histopathol 17 (2002) 715–720.

[15] L.J. Ko, C. Prives, p53: puzzle and paradigm, Genes Dev 10 (1996) 1054–1072.

[16] N.D. Lakin, S.P. Jackson, Regulation of p53 in response to DNA damage, Oncogene 18 (1999) 7644–7655.

[17] J. Langman, R.L. Guerrant, B.G. Freeman, Behavior of neuro-epithelial cells during closure of the neural tube, J Comp Neurol 127 (1966) 399–411.

[18] T. Miki, Y. Fukui, Y. Takeuchi, M. Itoh, A quantitative study of the effects of prenatal X-irradiation on the development of cerebral cortex in rats, Neurosci Res 23 (1995) 241–247.

[19] M. Muller, S. Wilder, D. Bannasch, D. Israeli, K. Lehlbach, M. Li-Weber, S.L. Friedman, P.R. Galle, W. Stremmel, M. Oren, P.H. Krammer, p53 activates the CD95 (APO-1/Fas) gene in response to DNA damage by anticancer drugs, J Exp Med 188 (1998) 2033–2045.

[20] K. Okamoto, D. Beach, Cyclin G is a transcriptional target of the p53 tumor suppressor protein, EMBO J 13 (1994) 4816–4822.

[21] K. Okamoto, H. Li, M.R. Jensen, T. Zhang, Y. Taya, S.S. Thorgeirsson, C. Prives, Cyclin G recruits PP2A to dephosphorylate Mdm2, Mol Cell 9 (2002) 761–771.

[22] D.H. Percy, Teratogenic effects of the pyrimidine analogues 5-iodo-deoxyuridine and cytosine arabinoside in late fetal mice and rats, Teratology 11 (1975) 103–117.

[23] E.J. Ritter, W.J. Scott, J.G. Wilson, Teratogenesis and inhibition of DNA synthesis induced in rat embryos by cytosine arabinoside, Teratology 4 (1971) 7–13.

[24] M. Selvakumaran, H.K. Lin, T. Miyashita, H.G. Wang, S. Krajewski, J.C. Reed, B. Hoffman, D. Liebermann, Immediate early up-regulation of bax expression by p53 but not TGF beta 1: a paradigm for distinct apoptotic pathways, Oncogene 9 (1994) 1791–1798.

[25] M. Ueno, K. Katayama, H. Nakayama, K. Doi, Mechanisms of 5-azacytidine (5AzC)-induced toxicity in the rat foetal brain, Int J Exp Pathol 83 (2002) 139–150.

[26] H. Yamauchi, K. Katayama, A. Yasoshima, K. Uetsuka, H. Nakayama, K. Doi, 1-β-D-Arabinofuranosylcytosine (Ara-C)-induce apoptosis in the rat fetal tissues and placenta, J Toxicol Pathol 16 (2003) 223–229.

[27] A.U. Zaidi, C. D'Sa-Eipper, J. Brenner, K. Kuida, T.S. Zheng, R.A. Flavell, P. Rakic, K.A. Roth, Bcl-X(L)-caspase-9 interactions in the developing nervous system: evidence for multiple death pathways, J Neurosci 21 (2001) 169–175.

Available online at www.sciencedirect.com
SCIENCE DIRECT®
Food and Chemical Toxicology 42 (2004) 1727–1736
www.elsevier.com/locate/foodchemtox

Morphological and microarray analysis of T-2 toxin-induced rat fetal brain lesion

Shinya Sehata [a,b,*], Naoki Kiyosawa [b], Toshihiko Makino [b], Fusako Atsumi [b], Kazumi Ito [b], Takashi Yamoto [b], Munehiro Teranishi [b], Yasuko Baba [a], Koji Uetsuka [a], Hiroyuki Nakayama [a], Kunio Doi [a]

[a] *Department of Veterinary Pathology, Graduate School of Agricultural and Life Sciences, The University of Tokyo, 1-1-1 Yayoi, Bunkyo-ku, Tokyo 113-8657, Japan*
[b] *Medicinal Safety Research Laboratories, Sankyo Co. Ltd., 717 Horikoshi, Fukuroi-shi, Shizuoka 437-0065, Japan*

Received 29 January 2004; accepted 15 June 2004

Abstract

To examine morphological and gene expression changes induced by T-2 toxin in the fetal brain in detail, pregnant rats on day 13 of gestation were treated orally with a single dose of T-2 toxin (2 mg/kg) and sacrificed at 1, 3, 6, 9, 12 and 24 h after treatment (HAT). Histopathologically, the number of apoptotic neuroepithelial cells in the telencephalon increased from 1 HAT and peaked at 12 HAT. Based on the histopathological examinations, microarray analysis was performed at 6, 12 and 24 HAT. Microarray analysis showed that the expression of oxidative stress-related genes (heat shock protein 70 (HSP70) and heme oxygenase (HO)) was strongly induced by T-2 toxin at 12 HAT, the peak time point of apoptosis induction. The expression of mitogen-activated protein kinase (MAPK)-related genes (MEKK1 and c-jun) and other apoptosis-related genes (caspase-2 and insulin-like growth factor-binding protein-3 (IGF-BP3)) was also induced by the T-2 toxin treatment. The changes observed by microarray analysis were confirmed for four up-regulated genes (HSP70, HO, IGF-BP3 and VEGF-A) using real-time RT-PCR. Our results suggest that the T-2 toxin-induced apoptosis in the fetal brain is due to oxidative stress, and that the MAPK pathway may be involved in T-2 toxin-induced toxicity.

Keywords: T-2 toxin; Rat; Fetal brain; Apoptosis; Microarray

1. Introduction

T-2 toxin is a trichothecene mycotoxin produced by various species of *Fusarium* spp. *Fusarium* spp. may be present in cereals including corn, oats, rice and wheat. T-2 toxin has been found to contaminate foods, animal foods and agricultural products, and has been reported in many parts of the world (WHO, 1990). A single or subacute dose of T-2 toxin induces damage in the lymphoid and hematopoietic tissues, resulting in lymphopenia and immunosuppression in many species (Hayes and Schiefer, 1982; Hoerr et al., 1981; Marasas et al., 1969; Pang et al., 1987; Shinozuka et al., 1998). These changes have appeared as apoptosis (Shinozuka et al., 1998; Sugamata et al., 1998). Furthermore, T-2 toxin has been shown to affect the central nervous system, but there have been no reported histopathological changes in the adult brain (Martin et al., 1986; Wang et al., 1998a; WHO, 1990). Wang et al. (1998b) also reported that the effect of T-2 toxin on blood brain barrier

* Corresponding author. Address: Medicinal Safety Research Laboratories, Sankyo Co. Ltd., 717 Horikoshi, Fukuroi-shi, Shizuoka 437-0065, Japan. Tel.: +81 538 42 4356; fax: +81 538 42 4350.
E-mail address: sehata@sankyo.co.jp (S. Sehata).

0278-6915/$ - see front matter © 2004 Elsevier Ltd. All rights reserved.
doi:10.1016/j.fct.2004.06.006

permeability, protein synthesis and monoamine oxidase activity might account for the neurochemical imbalance observed in T-2 intoxication. It is also reported that pregnant mice treated with T-2 toxin exhibited fetal death and fetotoxicity mainly in the central nervous and skeletal systems in addition to maternal toxicity (Ishigami et al., 1999, 2001; Rousseaux and Schiefer, 1987; Stanford et al., 1975). We have shown that apoptosis occurred in the fetal brain as in the thymus, liver, intestines, placenta and fetal liver at 24 and 48 h after treatment with T-2 toxin in pregnant rats on day 13 of gestation (Sehata et al., 2003). It is known that T-2 toxin induces lipid peroxidation, inhibits protein synthesis by interaction with ribosomes and inhibits DNA synthesis (Chang and Mar, 1988; Middlebrook and Leatherman, 1989; Thompson and Wannemacher, 1990). However, the mechanisms of T-2 toxin-induced changes, especially fetotoxicity, are not yet understood.

Recently, DNA Microarray technologies which allow one to detect the expression of many genes at the same time have been developed. The application of this technology to the field of toxicology, i.e. toxicogenomics, has been demonstrated. The expression of genes was reported in rats administered with hepatotoxicants, phenobarbital and carbon tetrachloride (Bulera et al., 2001; Waring et al., 2001). We have reported that T-2 toxin-induced transcriptional changes in the dam liver, placenta and fetal liver (Sehata et al., 2004). According to the results, similar changes in the expression of apoptosis-, lipid metabolism-, drug metabolizing enzyme- and oxidative stress-related genes were detected in these tissues, suggesting that oxidative stress might be involved in T-2 toxin-induced toxicity.

The purpose of the present study was to examine the detailed morphological changes and gene expression changes in the fetal brain obtained from pregnant rats treated with T-2 toxin. The protocol of this study was approved by the Animal Care and Use Committee of the Graduate School of Agricultural and Life Sciences, The University of Tokyo.

2. Materials and methods

2.1. Animals

Fifty-four pregnant Wistar:Slc rats (Japan SLC Co., Ltd., Hamamatsu, Japan) on day 11 of gestation (GD11) were obtained from Japan SLC Co., Ltd., Hamamatsu, Japan. The animals were kept using an isolator caging system (Niki Shoji Co., Ltd., Tokyo, Japan) under controlled conditions (23 ± 2 °C, 55 ± 5% humidity and a 14-h light/10-h dark cycle), and fed commercial pellets (MF; Oriental Yeast Co., Ltd., Tokyo, Japan) and water ad libitum.

2.2. Treatments

According to the results from the dose-finding study (data not shown) and a previously reported study (Sehata et al., 2003), the animals were used on day 13 of gestation (GD13). Eighteen animals were treated with a single oral dose of 2 mg/kg T-2 toxin (Sigma Chemical Co., St. Louis, MO, USA), and 3 animals were sacrificed for the histopathological examination by exsanguination under ether anesthesia at 1, 3, 6, 9, 12, and 24 h after treatment (HAT), respectively. For microarray analysis, based on the results of the histopathological examination, 9 rats were treated with T-2 toxin in the same way, and 3 rats were sacrificed at 6, 12 and 24 HAT, respectively. T-2 toxin was dissolved in corn oil and the dosing volume was adjusted to 2.5 ml/kg. In addition, a total of 27 animals which were treated with the vehicle alone were used as controls, and 3 animals were sacrificed at 1, 3, 6, 9, 12 and 24 HAT, respectively.

2.3. Morphological examination and immunohistochemical staining

After the animals were sacrificed, a macroscopic examination was performed. Fetuses were weighed. Fetuses from each dam were fixed in 10% neutral-buffered formalin to assess the changes induced by T-2 toxin. Paraffin sections of 4 μm were stained with hematoxylin and eosin (HE) and subjected to a microscopic examination. For the electron microscopic examination, the fetal brain was fixed with 2% glutaraldehyde/2% paraformaldehyde in 0.1 M phosphate buffer (PB) (pH 7.4) including 8% (w/v) sucrose for up to 96 h at 4 °C. The fetal brain was post-fixed with 2% osmium tetroxide in 0.1 M PB, and embedded in Poly/Bed 812 (Polysciences, Inc. Warrington, PA). Ultrathin sections were double-stained with uranyl acetate and lead citrate and observed under a JEM-2010 electron microscope (JEOL Ltd., Tokyo, Japan). Cells with fragmented DNA were detected by the TdT-mediated dUTP nick end labeling (TUNEL) method using an apoptosis detection kit (Apop Tag, Intergen, Purchase, NY, USA). In brief, multiple fragmented DNA-3′-OH ends on the section were labeled with digoxigenin-dUTP in the presence of terminal deoxynucleotidyl transferase (TdT). Peroxidase-conjugated anti-digoxigenin antibody was then reacted with the sections. Apoptotic nuclei were visualized by reacting with peroxidase-diaminobenzidine (DAB). The sections were then counterstained with methyl green. Morphometry was performed in the fetal brain (3 fetuses/dam) under a light microscope (×400). The number of positive cells/500 cells was counted and the mean ± SE of the three measurements was calculated. Statistical analysis was carried out by Student's *t*-test or Welch's *t*-test after analysis of homogeneity of variance by the *F*-test.

2.4. RNA extraction and microarray analysis

After the animals were sacrificed, fetuses were collected. Under a stereoscopic microscope, the fetal brain was collected and the tissue was frozen in liquid nitrogen as soon as possible. The frozen tissues were kept under −80 °C until the analysis was performed. Total RNA was extracted from frozen tissues using RNeasy Mini Kit (QIAGEN Inc., CA, USA). RNA from the fetal brain from each dam was pooled to generate a single sample, respectively. The quality of the RNA samples was checked by spectrophotometry according to the Affymetrix protocol. Microarray analysis (total 18 arrays) was performed according to the Affymetrix protocol at the sampling time points (6, 12 and 24 HAT) based on the results of the morphometrical examination. Briefly, cDNA was prepared from 5 μg of total RNA using the SuperScript Choice System for cDNA Synthesis (Invitrogen, CA, USA), with the exception that the primer used for the reverse transcription reaction was T7-$(dT)_{24}$ primer (Primer sequence: 5′-GGC CAG TGA ATT GTA ATA CGA CTC ACT ATA GGG AGG CGG-$(dT)_{24}$-3′, Amersham Biosciences, Tokyo, Japan). Following this, biotin-labeled cRNA was synthesized from the cDNA using the Enzo High Yield RNA Transcription Labeling Kit (Enzo Diagnostics, NY, USA). After 20 μg of biotin-labeled cRNA was fragmentated, a hybridization solution was prepared using GeneChip® Eukaryotic Hybridization Control Kit (Affymetrix) and hybridized to the Affymetrix Rat Genome U34A oligonucleotide array at 45 °C for 16 h in GeneChip® Hybridization Oven 640 (Affymetrix). The chips were washed and stained using the Fluidics Station (Affymetrix) and scanned with GeneArray® Scanner (Affymetrix).

2.5. Data analysis

The quality of the RNA samples used in the microarray analysis was checked by a 5′/3′ ratio of GAPDH housekeeping gene probes. The microarray imaging data were analyzed using Microarray Suite ver. 5.0 (Affymetrix) and Spotfire Pro Version 4.2 (Spotfire Inc., MA, USA) software. In brief, total array normalization (global normalization after trimming the top 2% and bottom 2% of the data) was performed in each experimental data (Yang et al., 2001). Probes containing at least one *Absence Call* in the data were also removed. We selected genes that gave a mean value of greater than +1.5 or less than −1.5. In addition, the mean value of each gene in the treated group was compared with that of the control group by Student's *t*-test or Welch's *t*-test after analysis of homogeneity of variance by the *F*-test. A significance level of $p < 0.01$ or $p < 0.05$ was considered acceptable.

2.6. Real-time RT-PCR

GeneChip® results were confirmed by real-time RT-PCR for selected genes such as heat shock protein 70 (HSP70), heme oxygenase-1 (HO-1), insulin-like growth factor-binding protein-3 (IGF-BP3), and vascular endothelial growth factor A (VEGF-A) (Table 1). Total RNA (5 μg) from each sample was prepared as described above. RNA was treated with 5 U of DNase I (Takara, Shiga, Japan) in the manufacturer's buffer containing 40 U RNase inhibitor (TOYOBO, Osaka, Japan) in a final volume of 50 μL, and subjected to phenol-chloroform purification. DNase I-treated total RNA of 2 μg was reverse transcribed in a final volume of 20 L using 200 U of Superscript II (Invitrogen, CA, USA) in the manufacturer's buffer containing 10 mM DTT, 0.5 mM dNTPs, and 40 U of RNase inhibitor. Real-time PCR was performed using qPCR™ Mastermix Plus (Eurogentec, PA, USA), and the transcription was quantified with a GeneAmp® 5700 Sequence Detection System (Applied Biosystems, CA, USA). For internal control, Rodent GAPDH Control Kit (Applied Biosystems) was used. Statistical analysis for the mean values was carried out by the *F*-test followed by Student's *t*-test or Welch's *t*-test.

Table 1
Sequences of oligonucleotide primer/probes used for real-time RT-PCR

Gene (GenBank#)	Primer		TaqMan® probe
HSP70 (Z27118)	Forward	TGGTGCAGTCGGACATGAA	CACTGGCCCTTCCAGGTGGTGAA
	Reverse	CGGGTAGAACGACCGGTTCT	
HO-1 (J02722)	Forward	TTCTTCTAGCGACAAGTTGATTCTGT	TCCTTGTACCATATCTATACGGCCCT
	Reverse	GCTTGTTTCGCTCTATCTCCTCTT	
IGF-BP3 (M31837)	Forward	TGCTGGGAGTGTGGAAAGC	AGGTTGTCCCCAGCACACATCGC
	Reverse	GAGTGGATGGAACTTGGAATCAG	
VEGF-A (U22372)	Forward	GGTCCCTCGTGGAACTGGAT	CGCCATTTTCTTATATTTGCTGC
	Reverse	CCGGGCTTGGCGATTT	